Only Copy

CASE FILE COPY

PI

From

1

The Pitot-static tube to be developed was intended to satisfy the following conditions: The pressure-velocity constant of the instrument was to be as near unity as possible, so that it could be used to determine both velocity and static pressure. The instrument was to be as little sensitive as possible to obliquity to the direction of flow, in order to give reliable measurements, even when the direction of flow is not known. The indications of the instrument were, moreover, to be as independent as possible of the more or less turbulent nature of the flow. Lastly, the geometric shape of the instrument was to be easily and accurately reproducible, so that it would not be necessary to calibrate each individual instrument. Moreover, it should be able to stand rough handling, in order to assure a uniform pressure-velocity constant and reliable measurements.

As to how successfully these requirements have been fulfilled, the following pages will show. Not all the experiments, which have contributed to the solving of the individual problems, will be described. Only for the ultimately established form, the Pitot-static tube of Prandtl, will it be shown as to how far the above stipulations have been met and brief descriptions will be given of only such intermediate experiments as are of practical importance.

II. - EXPERIMENTATION METHOD.

A Pitot-static tube can be employed in various ways. We may either employ an air current, in which the instrument is at rest, or the instrument itself can be made to move in straight or circular path through still air. The fundamental distinction between these two methods is not due to this difference (which, according to the laws of relative motion, is really no difference at all), but only to differences in the environment, which somewhat affect the experimental results. The first method was employed in most of the experiments under consideration, in so far as they related to a comparison of different instrument forms or to testing the same instrument at different angles to the direction of flow. The actual magnitude of the pressure-velocity constant was determined by calibration in circular motion. The results obtained in air naturally apply to other fluids.

For the comparative experiments, the ventilator plant of the Institute for Applied Mechanics of the Göttingen University and the wind tunnel of the Göttingen Aerodynamic Laboratory were placed at our disposal. The ventilator plant of the Institute is represented by Figs. 1 and 2. The Sirokko fan (driven, through a belt, by a 2 HP. shunt-wound motor) sucks the air, through a pipe of 300 mm inside diameter, from the room A and forces it back again into the same room. The entrance to this pipe from room A consists of a well-rounded funnel, in order to obtain the smoothest possible flow. Smoothing devices, such as "honeycombs" and wire gauze in front of the experiment section, hindered a uniform velocity distribution throughout the cross-section and were discarded after trial. Immediately in front of the fan there is a coarse honeycomb G, for the purpose of preventing reactions of the fan on the intake pipe. The pipe is gradually enlarged to about quadruple the cross-section at its exit end, so as to reduce as much as possible the velocity of the air reentering the room A. This room is, moreover, so large and the exit end of the pipe extends into it so far that the air comes completely to rest before being again drawn into the pipe. The suction pipe consisted of sheet-metal sections placed end to end, both to make as smooth a pipe as possible and to facilitate their removal, which was of special importance in the turbulence experiments. All joints were made tight with putty.

A mean velocity of 0 to 17 m/s could be obtained at will in the intake or suction pipe. This was roughly adjusted by changing the tension (220 and 440 volts) and the gear ratio between the motor and the fan and by partially closing the exit or pressure pipe by means of the valve S (Fig. 1). A rheostat in the field of the motor served for the fine adjustment and maintenance of the desired revolution speed in opposition to tension variations in the circuit and the effect of the heating of the motor. For testing the uniformity of the air flow, the pressure drop in the intake pipe as compared with the pressure in the room A was measured and was found to be proportional to the square of the quantity of air drawn in. The adjustment was originally made by hand in accord with the indications of the control manometer, but it was subsequently made with the aid of an automatic pressure regulator built on the principle of a manometric balance. (Regarding the details of this pressure-regulating device, see Kröner, "Versuche über Strömungen in stark erweiterten Kanalen," Forschungsarbeiten auf dem Gebiete des Ingenieurwesens, No. 222, published by the Society of German Engineers, Berlin, 1920.)

A rotatable section K (Figs. 1, 3 & 4), provided with a scale, served for the reception of the Pitot-static tube. The Pitot-static tube could be easily shifted in this section in the direction of the diameter and turned about the axis of the spindle. This was generally done between the limits of +50 and -50°. The rotatable section was located about 1.6 m back of the intake funnel. The distribution of the pressure in the horizontal plane, in which the Pitot-static tubes were turned, was very uniform (Fig. 5). In the middle third of the pipe the deviation in the pressure, compared with that measured at the axis, was, at the most, 0.25%, so that the observed pressure deviations were really due to the obliquity of the Pitot-tube and not to any local differences in velocity. Control tests were also made in a rectangular channel, in which the nose of the Pitot tube, by transverse and longitudinal motions of the rotatable section, could be kept continuously at the same point in the channel. The curves thus obtained agreed perfectly with those obtained in the above manner.

NATIONAL ADVISORY COMMITTEE FOR AERONAUTICS.

TECHNICAL MEMORANDUM NO. 303.

PITOT - STATIC TUBES FOR DETERMINING THE VELOCITY OF AIR.*

By H. Kumbruch.

I. - INITIATION AND PURPOSE OF THE EXPERIMENTS.

On the occasion of the formulation of the rules for testing the efficiency of ventilators and compressors, experiments were instituted by the subcommittee on ventilators for the production of suitable tubes for velocity and pressure measurements. The investigation was entrusted to Professor Prandtl in Göttingen, who had already done work of this character, and was financially supported by the Society of German Engineers (Verein deutscher Ingenieure). The experiments extended through a number of years, partly because the initial measurements were made with technically inadequate apparatus. Moreover, the field of investigation was subsequently enlarged by the introduction of the newly invented Pitot-static tubes of Professor Brabbée, Charlottenburg, and of the Georg Rosenmüller firm, Dresden, as also of two older baffle-plate forms for comparative experiments.

I am greatly indebted to Professor Prandtl for his frequent suggestions and assistance in carrying out the experiments. My thanks are likewise due to the Society of German Engineers for its financial support.

* From "Forschungsarbeiten auf dem Gebiete des Ingenieurwesens," 1921, No. 240.

In order to determine the effect of the spindle on the pressure indications of the Pitot-static tubes, they were also turned about the transverse axis perpendicular to the spindle. These experiments were performed in the old wind tunnel, as shown diagrammatically in Figs. 6 & 7. (Prandtl, "Die Bedentung von Modellversuchen für die Luftschiffahrt und Flugtechnik," Zeitschrift des Vereins deutscher Ingenieure, 1909, p. 1711.) An octagonal nozzle of 1015 mm inside diameter was placed in the 2 x 2 m tunnel. By this reduction in the size of the air stream a very uniform velocity distribution throughout the cross-section was obtained. The Pitot-static tubes were placed about one meter in front of the nozzle. The supporting frame and the circular scale for adjusting the apparatus lay outside the air stream. The apparatus was turned from 45 to -45°.

Two Krell micromanometers (Fuess type), with alcohol filling, served for all the pressure experiments. They were calibrated by successive additions of known quantities of alcohol. For greater inclinations, a pipette sufficed for the determination of these quantities, the specific gravity being determined by means of a specific gravity bottle. The greater or less agreement of the scale divisions, found for the individual steps, furnishes an indication of the quality of the vertical tube as regards its calibration and straightness. In fan and turbulence experiments, the same conversion ratio could be used in the computations for every inclination employed. For the calibration of the very flat positions sometimes employed in whirling experiments (e.g., an inclination of 1 : 70

with a manometer placed in the direction of the wind), the quantity of fluid was weighed and allowance made for even slight variations of the conversion ratio above the vertical height.

The special devices employed for the turbulence and whirling-arm experiments, including the method of calibration, are described farther on.

III. - THEORY OF PITOT-STATIC TUBES.

Velocity measurements with Pitot-static tubes consist in finding the difference between the pressure on the nose and on the smooth lateral walls of an immersed solid of revolution, whose axis is parallel to the direction of flow. The pressure on the nose is the resultant of the dynamic pressure $(q = \gamma\ v^2/2g)$ and static pressure. The pressure on the lateral portion of the surface is the sum of the static pressure and of a negative pressure cq proportional to the dynamic pressure. The difference of these two pressures is independent of the magnitude of the static pressure and is therefore proportional to the dynamic pressure. It is

$$p_1 = (1 + c)\ q = \beta\ q$$

in which β is the pressure-velocity constant of the Pitot-static tube. Both c and β depend on the location of the measuring point on the lateral surface of the cylinder (Blasius, "Ueber verschiedene Formen Pitotscher Röhren," Zentralblatt der Bauverwaltung, 1909). The pressure distribution on a revolution solid can be calculated in certain cases according to the principles of hydrodynamics (potential motion). The simplest case for this purpose is that of the conoid created by the superposition of a parallel flow and the flow from a concentrated source (Fig. 8). The surface (or curve s in the figure) separates the outer and inner flow. It is identical with the meridian of the conoid. The curve a shows the pressure distribution on this conoid. The static pressure is assumed to be zero and the pressure p is given in fractions of the dynamic pressure of the flow at infinity $q_0 = \gamma v_0^2/2g$. At the tip of the nose, where the velocity is zero (center of dynamic pressure or separation point), there is the full dynamic pressure. Laterally from this point, the pressure falls rapidly, passes through zero, reaches its minimum value (which, on the conoid, is 1/3 of the dynamic pressure) and asymptotically approaches the pressure of the undisturbed flow. At a distance of about 3d from the center of the nose (d = the thickness of the conoid at infinity) the negative pressure on the wall of the conoid is 2% of the dynamic pressure. In reality, it is never a question of strict potential motions. The flow itself is mostly turbulent and is made more turbulent by the introduction of the Pitot tube, but the computed and actual pressure distributions have been found to agree very well for the portion of the conoid involved in the experiment under consideration. (G. Fuhrmann, "Theoretische und experimentelle Untersuchungen an Ballonmodellen," Jahrbuch der Motorluftschiff-Studiengesellschaft, 1911-1912.) The deviations first become noticeable at the rear end of the conoid.

IV. - PRANDTL'S PITOT-STATIC TUBE.

1. Old form.- Figs. 9 and 10 show the first Pitot-static tube constructed on this principle.* Its nose is somewhat more pointed than the conoid just considered (about half a revolution ellipsoid with an axis ratio of 1 : 2). The pressure distribution along the revolution solid is not thereby affected. To the nose (of diameter d) there is joined the cylindrical portion of the tube with four perforations, at a distance of 4.3 d from the tip, for the determination of the static pressure. This instrument partially fulfills the conditions mentioned in the introduction. Up to an angle of about 17° to the direction of flow, it gives the full dynamic pressure (Fig. 11). Here, as in all subsequent similar diagrams, the deviations in the individual pressure readings, when the instrument is inclined to the direction of flow, are always shown in hundredths of the dynamic pressure at the zero position, when the axis of the Pitot-static tube is parallel to the direction of flow. The velocities at which the experiments were performed are noted on the diagrams. The relative error is independent of the magnitude of the velocity. The error indicated for the dynamic pressure relates to the square of the velocity. The error in the velocity itself is therefore, for small inclinations of the axis of the instrument to the direction of flow, only half as large as for the recorded dynamic

* This instrument is described in the "Mitteilungen der Prüfungsanstalt für Heizungs-und Luftungseinrichtungen," Charlottenburg, No. I.

pressure.* The error in the dynamic pressure at 20° is -2% and at 30° it is about 16.5% of the reading in the zero position.

The behavior of the rear perforations in the oblique flow is likewise very favorable. The deviations in the static pressure are, for small inclinations, somewhat greater than those of the dynamic pressure, but smaller than the corresponding errors obtained with most of the instruments yet to be described. The pressure-velocity constant of the Pitot-static tube is 1.013, i.e. practically 1.

2. New form.- In spite of its very favorable characteristics, this form was subsequently abandoned, chiefly because of the difficulty of accurately reproducing the shape of the nose. It was replaced by the Pitot-static tube shown in Figs. 12-14. To the cylindrical portion there was joined, instead of the semi-ellipsoid, a hemispherical nose of diameter d. The other dimensions are based on this quantity d, in so far as they affect the manner of functioning of the instrument. The nose has a cylindrical passage of diameter $b = \sim 0.3\ d$ and a depth of at least 2 d. The best bore was determined by experiment. Figs. 15-16 show the effect of three different bores on the dynamic and static pressure. For bores smaller than 0.3 d the dynamic pressure in an oblique position falls more rapidly, but for greater bores it shows a depression whereby

* This ratio is obtained by the binomial development of the expression $\sqrt{1 + x}$, which gives $\sqrt{1 + x} = 1 + \frac{x}{2} + \frac{x^2}{8} + \ldots\ldots$
If the series is broken off after the linear term in x, the ratio utilized is obtained.

the error first climbs to barely 4% at 16° inclination and then falls. The static pressures are practically equal for all three bores. The dissymmetry for the instrument with normal bore may be due to inaccuracies of shape. The experiments were not performed with the same instrument by increasing the size of the bore, but with three different instruments, since they had to be used again for the turbulence experiments. Instead of the four rear perforations, there was a slot extending entirely around the tube, in order to afford symmetrical relations toward all sides for slight deviations in direction. This slot was located about 3 d back of the nose. According to Fig. 8, the pressure was already approximately static at this point. A further diminution of this distance, which might be desirable for a locally disturbed flow, would increase the pressure-velocity constant of the instrument, due to the increasing negative pressure toward the nose, and make it more sensitive to turbulence. Any increase in the distance beyond 3 d, however, does not give any considerable improvement in either direction. The width of the slot was about 0.1 d. Too wide a slot increases the pressure-velocity constant of the Pitot-static tube somewhat, by increasing the suction of the passing air and makes it chiefly dependent on the internal structure of the tube. In the oblique position, the width of the slot has practically no effect on the measurement of the difference. In order to eliminate the effect of the spindle (which contains the pipes serving to transmit the pressure from the nose and slot) on the pressure readings, the distance between the slot and spindle should be 8 to 10 δ, in which δ represents the thickness of the spindle. A less distance makes the pressure distribution on the slot unsymmetrical and increases the pressure measured in the middle of it. The spindle is pressed flat, in order to diminish as much as possible the disturbance caused by it. How far forward the effect of the spindle extends, can be easily determined for a cylindrical conoid, by calculating the loss in velocity on the axis as far as the center of dynamic pressure (v = 0 m/s) and therefrom the pressure increase according to the equation of Bernoulli. Fig. 17 gives the pressure for a laterally infinite conoid ("even problem"), hence for a Pitot-static tube with double spindle. With a one-sided spindle we can make the mean pressure increase at the slot only half as great. The distance of 8-10 δ applies to a one-sided spindle. The pressure increase at the distance of 10 δ is about 3% of the dynamic pressure. This increase serves to offset the negative pressure at the slot. If there is another spindle, as is often the case with instruments for very large pipes, then, with otherwise like dimensions of the conoid, the distance between slot and spindle must be 18 to 20 δ, if the coefficient of the Pitot-static tube is to remain 1. In the latter case, however, we can move the slot nearer to the nose, in order to avoid increasing the length of the conoid. In this case the distance between the two must be about 1.7 d.

Of the inner mechanism of the Pitot-static tube, only that portion is important, which receives the pressure of the slot. When the instrument is inclined to the direction of flow, there is no continuous equilibrium inside, but the air flows through the slot. In order that no chance intermediate value may be measured in this flow, the slot first opens internally into a chamber, in which the pressure can reach a state of equilibrium. The tubes for transmitting the slot pressure terminate in this chamber. It is very important for the correct functioning of the slot, that its edges shall be accurately shaped. Careful attention must be given this matter in making the instrument.

Figs. 18-19 show the behavior of the Pitot tube in the inclined position. For the above-mentioned reason, the instrument was turned about both its spindle axis and its transverse axis. The indications of the Pitot-static tube, in the measurement of the pressure difference, were affected on the one hand by the behavior of the bore in the nose and, on the other hand, by the slot. Both were tested separately and had to be so shaped as to make the pressure changes equal for as large an angle as possible, in order for the difference measurement within this angle to give constant values.

The pressure data of the nose are given only for the transverse turning. Like curves are obtained by turning about the spindle. The resultant pressure falls with increasing obliquity. This is easily explained. The center of dynamic pressure lies in the zero position, i.e., the position of maximum pressure at the apex of the sphere and hence in the orifice. On turning the nose, it is shifted laterally near the orifice, while the latter is itself shifted into a region of lower pressure (Compare "Druckverlauf um eine Kugel" by O. Krell, Jr., in "Ueber Messung von dynamischem und statischem Druck bewegter Luft," Munich, 1904, p. 41).

In the oblique position, the slot likewise shows a pressure decrease (increase of negative pressure). This is not so easily explained as in the case of the nose. It comes from the combined action of different causes. If the slot is far enough back of the nose (whose shape is immaterial for this discussion), the pressure, in the axial position, is then approximately static on the whole circumference of the slot. If, however, the Pitot-static tube is oblique to the direction of flow, the pressure distribution on the slot becomes uneven. On the side toward the flow there is positive pressure and on the back side negative pressure or diminished positive pressure and in the intervening regions, in part, greater negative pressure. This pressure distribution produces a turbulent flow about and through the slot and it is obvious that the resulting slot pressure, measured by the manometer, is smaller than the static pressure. The above-mentioned chamber was provided for the purpose of equalizing the pressure between the different positions of the slot.

Figs. 18-19 show the deviations in detail. The velocity is correctly given up to 15° inclination. At 20° the error in the velocity calculated from the dynamic pressure amounts to a mean of

-1.9%; at 30°, -10.5% of the axial velocity. The deviations in static pressure are greater. The tube gives accurate results only in the zero position or within a few degrees of it. It is to be noticed, first of all, that, in the inclined position, the tube gives too small a pressure, hence too great a negative pressure in the case considered. At 10° the error in the static pressure is -1.8%; at 20°, -8%; and at 30°, -16% of the axial dynamic pressure. These errors in the pressure readings of the slot are somewhat smaller, if the edges of the slot are rounded off. Figs. 20-21 give the curves of dynamic and static pressure of a Pitot-static tube, first with square and then with rounded edges, the rounding radius being about 0.5 mm. The difference is here particularly noticeable, since the instrument with a square-edged slot, for reasons not accurately determined, shows a greater sensitiveness of the slot to direction, than the instrument with which Figs. 18-19 were obtained. The diminished direction sensitivity of the slot with the rounded edges affects the difference measurement unfavorably. The following table compares the two instruments.

Table I.

	Error in % of dynamic pressure				
	Dynamic pressure		Static pressure		
	20°	30°	10°	20°	30°
Slot edges square	-2.8	-15	-3.2	-11.3	-23.4
Slot edges round	-4.4	-25	-0.7	- 6.3	-11.7

The effect of the one-sided spindle made itself felt in a practically insignificant dissymmetry of the pressure curves obtained by turning about the transverse axis. The errors given for direction deviations are mean values from the data for turning about the spindle and transverse axis.

3. Special forms of Prandtl's Pitot-static tube.

a) Dust instrument.- Special forms of the Pitot-static tube were made for special purposes, which differed from the normal form chiefly on the inside. For experiments with air currents containing dust, an enlargement of the normal form (d = 12 mm) was utilizable. Practical experiments showed it to be expedient to close the front opening loosely with cotton wool, which did not hinder the pressure transmission, in order to prevent the soiling of the inside of the tube. On the rear end, there was a screw plug to facilitate the cleaning of the inside.

b) Mine instrument.- For measurements in moist and very impure air, e.g., in mines, an instrument is used with greatly increased dimensions, d = 55 mm diameter (Figs. 22-24). The front orifice opens into a chamber where the condensed water and foreign bodies can be deposited. The pressure-transmission pipe is inclined, in order to facilitate the exit of the condensed moisture. For this purpose, the support a rests, during the experiment, on a water seal. The slot does not go clear around, but there are, for structural reasons, four interruptions left in the circumference of the outside pipe. For transmitting the pressure, pipes or hose connections can be screwed into the coupling boxes b. Otherwise, the dimensions of the instrument correspond to the proportions of the normal form. Fig. 25 shows the direction sensitivity for the pressure difference and slot-pressure measurement. Contrary to the normal form, this instrument, in the inclined position, first shows a slight increase in the dynamic pressure, up to 2% error, which is apparently connected with the greatly enlarged dimensions. It seems probable that (due to the law of similitude for viscous fluids) the small instruments tested at very high velocities will show similar deviations.

c) Component instrument.- It may occasionally be desired to measure the components of the flow velocity in a given direction. Such, for example, is the case, when it is desired to determine the quantity of air flowing through a cross-section in an oblique direction, without knowing the angle of inclination α between the flow-direction and the perpendicular to the cross-section. The velocity component in question is $v \cos \alpha$. In order to determine this value, we need a Pitot-static tube, which, placed obliquely at the angle α, will give the value $\frac{\gamma v^2}{2\ g} \cos^2\alpha$ as the pressure difference. It will probably be difficult to make an instrument which will meet this requirement for any desired angle. Within a comparatively small angular range, the component measurement can be made with a normal Pitot-static tube, having a nose orifice of about 0.1 d. Fig. 26 gives the deviations in the pressure data, as compared with the theoretical value $\frac{\gamma v^2}{2\,g}\cos^2\alpha$, for two bores of 0.15 d and 0.06 d. The differences between the measured and calculated velocity are shown in Table II. With the instrument having the larger bore, the pressure data fall slower than would correspond to the cos curve. On the contrary, the tube with the smaller bore shows too little pressure from the beginning.

Table II.

Inclination	Error of measured velocity in % of calculated velocity component.						
	10°	15°	20°	25°	30°	35°	40°
b/d = 0.061	-0.2	-0.6	-0.8	-1.7	-4.1	-6.5	-8.4
b/d = 0.156	+ 0.5	+0.9	+0.2	+0.3	-1.9	-4.6	-9.0

The best bore for component measurement is probably about 0.1 d.

V. - TESTING FOREIGN FORMS OF PITOT-STATIC TUBES.

The object of the investigation, aside from the creation of an extensively utilizable and reliable Pitot-static tube, was to make comparative tests of tubes from other sources, especially those of Brabbée and of G. Rosenmüller, Dresden.

1. Brabbée's Pitot-static tube.- This tube is already known through the "Mitteilungen der Prüfungsanstalt fur Heizungs- und Lüftungseinrichten," No. 1. In design, it reminds us of the old Pitot-Darcy tube (Rühlmann, "Hydromechanik" 2d edition, Hannover, 1879) and of the American forms (Gregory, "The Pitot Tube," Trans-

actions of the American Society of Mechanical Engineers, 1904; Taylor, "A form of Pitot Tube for measuring air velocities," English News, 1903). It consists of two concentric cylindrical tubes with the same axis and a cone for the transition from the inner to the outer tube. The inner tube projects a distance equal to its own diameter beyond the outer tube (Figs. 27-29). The static pressure is measured through four perforations in the outer tube. The tube we used had an outside diameter of 7 mm.

Figs. 30-31 show the effect of inclining the tube to the direction of flow on the pressure readings for revolution about the spindle and transverse axes. The nose shows the known pressure distribution of a tube cut off square. The resultant pressure remains constant up to about 15°, so long as the center of dynamic pressure lies in the orifice. With greater inclinations, the suction effect of the air flowing by the orifice creates a noticeable diminution in the pressure. With the inclination of the tube, the static pressure falls quite rapidly from the start. Consequently, the dynamic pressure measurements give too high values (up to about 10% of the axial dynamic pressure), so long as the resultant pressure remains constant. The error in the dynamic pressure is zero, where the resultant and the static pressure show the same deviation as a result of the obliquity (about 40°). The effect of the spindle produces a slight dissymmetry in the distribution of the static pressure and consequently also of the dynamic pressure. The pressure-velocity constant of the instrument is

1.001, i.e., practically 1. Hence, the instrument correctly indicates the static pressure in the zero position.

There are also several special forms of the Brabbée Pitot-static tube.* A tube of d = 13 mm diameter, which has six slots 1 x 3 mm, instead of the four holes, shows about the same sensitivity to inclination. The same holds true for another tube, which serves only for measuring static pressure. The inner tube is cut off at the front end of the cone and closed at its base. The external pressure is relieved by two rows of four slots 0.5 x 10 mm, which in the longitudinal direction are about 10 mm apart and transversely 45° apart.

3. Rosenmüller's Pitot-static tube.- This instrument closely resembles the new form of Prandtl's Pitot-static tube. It likewise has a hemispherical nose (Figs. 32-34). The principal dimensions, based on the diameter d of the nose, are: nose bore, b = 0.245d; distance of slot from tip of nose, 2.8 d; width of slot, 0.1 d; distance of spindle behind slot, 8.4 δ(δ = thickness of spindle). The front edge of the slot is rounded. The slot is covered on the spindle side for a width of about 0.5 d, in order to prevent any reaction of the spindle on the pressure readings of the slot. The rear end of the instrument forms a cone, in order to avoid too great turbulence behind it. This cone has no effect on the pressure readings of the Pitot-static tube. Its introduction into the pipes is difficult and requires comparatively large openings.

* ("Erlanterungsbericht zu den Regeln fur Leistungsversuche an Ventilatoren und Kompressoren" V.D.I., 1912, p. 1834, Fig. 15.)

The pressure data of the nose (Figs. 35-36) show nothing new for inclined positions. The static pressure, while turning about the spindle axis, falls more slowly than with the Pitot-static tubes of Prandtl and Brabbée. Through the interruption in the slot, the region of strong negative pressure in the oblique position does not arise on the one side; the mean pressure is greater and, hence, the error is smaller than with the slot extending the whole distance around. This result is partly due to the rounding of the front edge of the slot. In the difference measurement, this causes the falling off to begin somewhat sooner (at about 10°) than with Prandtl's Pitot-static tube (about 15°). In turning about the transverse axis, the interruption in the slot produces an undesirable effect, in that it renders the distribution of the static pressure entirely unsymmetrical in the oblique position. If the interruption in the slot is turned toward the oncoming air stream, then the negative pressure takes effect only on the side and rear. The positive pressure on the front side does not take effect and the instrument accordingly indicates too small a static pressure. On turning toward the other side, the positive pressure is eliminated on the rear side, so that the air cannot flow through the slot, but is stopped by the interruption in the slot and the static pressure measures too great. This lack of symmetry naturally affects the distribution of the dynamic pressure also. The lack of perfect symmetry in the distribution of the resultant pressure may be due to a slight deviation of the nose of the semiconical form. The manner of functioning of the instrument would be better without than with the slot covering. It is not needed to prevent the reaction of the spindle, since, for the dimensions chosen, the reaction of the spindle on the slot is just about great enough to offset the positive pressure on the slot. The thick round spindle is also of doubtful advantage, since, as a result of the constriction, it renders the velocity distribution in the test cross-section very unsymmetrical. The coefficient of the instrument is 0.992 and may be considered as 1 for all practical purposes. This Pitot-static tube can also be employed parallel to the direction of flow for measuring the static pressure.

Before the invention of the form of Pitot tube described, Recknagel's baffle plate was extensively employed with the pressure-velocity constant of 1.37 found by Recknagel ("Zeitschrift des Vereines deutscher Ingenieure," 1886, p.489). Rietschel's experiments demonstrated the inaccuracy of this constant and, moreover, called attention to the dependence of the coefficient on the flow characteristics.* In order to settle this beyond dispute, two baffle plates were also employed in the turbulence experiments described in the following section (Figs. 37-39). One had a rectangular cross-section and a thickness of 5 mm; the other, semicircular edges and a thickness of 3 mm. In turning, the round-edged baffle plate behaved better than the one with square edges (Fig. 40).

It may be well here to make brief mention of experiments intended to give information as to how far a baffle plate, placed in

* ("Mitteilungen der Prüfungsanstalt für Heizungs- und Lüftungseinrichtungen," Charlottenburg, No. 1.)

the direction of flow, is adapted for measuring static pressure. Fig. 41 shows the experimental arrangement in the old wind tunnel of the Göttingen laboratory. A Prandtl Pitot-static tube of normal form served for comparison. Both instruments were in a region of uniform velocity and were located only far enough apart, so they could not disturb each other. The baffle plate was first placed parallel to the direction of flow, i.e., so that both perforations showed the same pressure. Then this pressure was compared with that of the Pitot-static tube and finally the flow velocity was measured with the latter. Due to the suction effect of the air flowing by, both baffle plates showed negative pressure. For the baffle plate with rounded edges, the suction effect was about 11% of the velocity. For the square-edged baffle plate, the suction effect fell from about 54 to 23% (Fig. 42 and Table III). Similar results were obtained with other baffle plates, such as lens-shaped plates, flattened lenses or rounded disks with more or less depressed middle portion. It is not necessary to go into further details concerning baffle plates, since Pitot-static tubes, on account of their greater convenience and reliability, are now generally preferred.

Table III.

Pressure measurements with obliquely placed baffle plates.

Baffle plates with round edges.

Dynamic pressure q mm water	Velocity v m/s	Pressure difference split disk mm water	Pressure difference split disk % of q
0.93	3.85	0.13	14.0
1.33	4.61	0.15	11.3
1.72	5.25	0.20	11.6
2.13	5.84	0.24	11.3
2.56	6.40	0.29	11.3
2.96	6.38	0.33	11.2
3.36	7.33	0.37	11.0
3.78	7.78	0.45	11.8
4.24	8.24	0.49	11.5
4.67	8.65	0.50	10.7
5.14	9.08	0.57	11.1
5.59	9.46	0.60	10.7

Baffle plates with square edges.

Dynamic pressure q mm water	Velocity v m/s	Pressure difference split disk mm water	Pressure difference split disk % of q
0.89	3.77	0.47	52.8
1.44	4.80	0.78	54.1
2.02	5.69	1.08	53.5
2.62	6.48	1.32	50.4
3.22	7.18	1.45	45.0
3.86	7.85	1.54	39.9
4.47	8.46	1.49	33.3
5.10	9.03	1.45	28.4
5.76	9.60	1.35	23.5

VI. - EFFECT OF DEGREE OF TURBULENCE OF AIR STREAM ON READINGS OF PITOT-STATIC TUBES.

The Report of the Testing Laboratory for Heating and Ventilating Devices (Bericht der Prüfungsanstalt für Heizungs- und Luftungseinrichtungen) already referred to, first calls attention to the dependence of the indications of a baffle plate on the nature of the air flow. Any accurate and hence quantitative determination of the velocity is impossible with this instrument. Therefore it was required of the new Pitot-static tube that its readings should be affected in the least possible degree by the turbulence of the air. In this connection, the term "turbulent" will not be employed in the usual sense of opposition to "laminar," since, in the technically occurring air motions, we would probably never have to do with laminar currents, i.e., with currents below the critical velocity. The term turbulent is here intended to apply to a current containing strong eddies and consequently of varying direction.

The effect of the turbulent nature of the flow on the readings of the Pitot-static tube can be most readily determined by measuring the dynamic pressure at different points in the tunnel both in a smooth and in a turbulent current and comparing the results. This comparison is rendered difficult by the fact that individual measurements are not accurate in very turbulent currents. The following method, though slower, is more accurate. The quantity of air drawn in is determined by velocity measurements throughout the cross-section in a smooth current (i.e., directly behind the entrance cone) and then in a very turbulent current. The unreliableness of any single measurement still persists, but the mean of several measurements is accurate enough to enable a reliable comparison, as will be further demonstrated. Special disks (Figs. 43-44) were employed in the entrance pipe 2.25 m in front of the test point for creating especially turbulent currents.

If $q_o = \beta_o \frac{\gamma v_o^2}{2g}$ denotes the measured pressure difference in a smooth current; β_o, the pressure velocity constant of the Pitot-static tube in a smooth current; $q_1 = \beta_1 \frac{\gamma v_1^2}{2g}$, the measured pressure difference in a turbulent current; β_1, the pressure-velocity constant of the Pitot-static tube in a turbulent current; and R, the radius of the conducting pipe, then the quantity of air flowing through the pipe in a smooth current is

$$Q = 2\pi \int_0^R v_o \, r \, d\, r \quad \text{or, since} \quad v_o = \sqrt{\frac{2g}{\gamma} \frac{q_o}{\beta_o}}$$

$$Q = \pi \sqrt{\frac{2g}{\gamma \beta_o}} \int_0^R \sqrt{q_o} \, d(r^2).$$

For the same quantity of air in a turbulent current,

$$Q = \pi \sqrt{\frac{2g}{\gamma \beta_1}} \int_0^R \sqrt{q_1} \, d(r^2) \quad \text{and, hence,}$$

$$\sqrt{\frac{1}{\beta_o}} \int_0^R \sqrt{q_o} \, d(r^2) = \sqrt{\frac{1}{\beta_1}} \int_0^R \sqrt{q_1} \, d(r^2) \quad \text{or}$$

$$\frac{\beta_1}{\beta_o} = \frac{\int_0^R \sqrt{q_1} \, d(r^2)}{\int_0^R \sqrt{q_o} \, d(r^2)}$$

and hence the ratio of the pressure-velocity constants is

$$\frac{\beta_1}{\beta_c} = \left[\frac{\int_c^R \sqrt{q_1}\, d(r^2)}{\int_c^R \sqrt{q_0}\, d(r^2)}\right]^2$$

If q is already the mean dynamic pressure on the surface of the ring (of diameter r) and if we place the mean value of q over R_2, then the surface (called the "volume-surface" V) giving the expression $\int \sqrt{q}\, d\, r^2$ is proportional to the quantity of air delivered. For the most accurate possible determination of the mean value of the dynamic pressure on the ring surfaces, the Pitot-static tube to be tested was mounted in a rotatable section D (Figs. 1, 45 and 46). The Pitot-static tube can be shifted in the radial direction in the rotatable section. The latter forms an integral portion of the intake pipe, runs into two rings R screwed to a frame and can be turned about the axis of the rings. The rotary motion of the section is transmitted by a string to the drum of the recording mechanism of a micromanometer (Prandtl, V.D.I. 1909, p. 1716, Fig. 11). The power transmission between the rotatable section and the recording drum is so adjusted, that one revolution of the section causes one revolution of the drum. Thus the deflection of the manometer is recorded on the unwound circular path of the Pitot-static tube. Fig. 47 shows a diagram obtained in this manner, of which each Pitot-static tube gave nine specimens, corresponding to the three flow conditions and the three mean velocities 6, 9.5 and 13 m/s. From these diagrams the mean dynamic pressure for each ring was determined by planimetry. The local variations in dynamic pressure on the same ring are sometimes quite large, especially at high velocities and in a turbulent air stream. Nevertheless the mean values of the repeated records agree very satisfactorily, the deviations being mostly less then 1%, showing that the results of this method are more accurate than those obtained by the method mentioned at the beginning of this section, which was based on the comparison of the individual local measurements. Figs. 48-49 likewise illustrate the accuracy of the mean velocities thus obtained. The mean measured dynamic pressures, on account of the varying diminution of the cross-section by the spindles of the different Pitot-static tubes, were always recalculated with the aid of the continuity equation, on the basis of a clear cross-section of the pipe.

Table IV.

Prandtl's Pitot-Static Tube.

Without turbulence disk. Volume surface V_0 cm²	With turbulence disk I: Volume surface V_1 cm²	With turbulence disk I: Ratio of coefficients $\frac{\beta_1}{\beta_0} = \left(\frac{V_1}{V_0}\right)^2$	Mean % increase in coefficient due to turbulence	Remarks	
175.6 263.4 395.1	178.6 269.5 403.6	1.034 1.046 1.044 1.041	4.0	Normal bore	Square-edged slot
176.7 264.0 395.0	178.7 269.7 404.7	1.022 1.043 1.051 1.039	3.9	Wide bore	Square-edged slot
175.6 263.4 394.5	176.8 267.1 400.7	1.014 1.028 1.028 1.023	3.1	Narrow bore	Square-edged slot
166.0 263.2 367.0	169.4 270.8 377.9	1.040 1.059 1.059 1.053	5.2	Normal bore with round-edged slot.	

Table IV (Cont.)

Prandtl's Pitot-Static Tube.

Without turbulence disk. Volume surface V_0 cm²	With turbulence disk II: Volume surface V_2 cm²	With turbulence disk II: Ratio of coefficients $\frac{\beta_2}{\beta_0} = \left(\frac{V_2}{V_0}\right)^2$	Mean % increase in coefficient due to turbulence	Remarks	
175.6	178.5	1.033			Square-edged slot
263.4	268.5	1.040	4.0	Normal bore	Square-edged slot
395.1	402.4	1.041			Square-edged slot
		1.038			
176.7	177.9	1.014			Square-edged slot
264.0	270.8	1.053	3.9	Wide bore	Square-edged slot
395.0	402.1	1.036			Square-edged slot
		1.038			
175.6	177.6	1.022			Square-edged slot
263.4	268.3	1.038	3.1	Narrow bore	Square-edged slot
394.5	403.4	1.046			Square-edged slot
		1.039			
166.0	169.6	1.044			
263.2	270.7	1.057	5.2	Normal bore with round-edged slot.	
367.0	376.2	1.051			
		1.051			

The results of the turbulence experiments are given in Tables IV and V. The corresponding volume surfaces of an instrument were always recalculated on the basis of equal pressure drop in the funnel (equal quantities delivered). The differences in the volume surfaces for the classified flow conditions for the different Pitot-static tubes aside from the different values of the pressure-velocity constant, are due to unavoidable errors in the frequent adjusting of the same rate of flow with the pressure regulator. No calculations were attempted in this connection, since the accuracy of the measurements for finding or verifying the pressure-velocity constant was not great enough. The Pitot-static tubes all showed an increase in their pressure-velocity constant in a very turbulent air stream, their mean values being

for Prandtl's	Pitot-static tube with normal bore,	4.0%
" "	" " " " wide "	3.9"
" "	" " " " narrow "	3.1"
" "	" " " " rounded slot	5.2"
" Brabbee's	" " "	5.4"
" Rosenmüller's	" " "	4.2"
" the baffle plate with round edges		10.6"
" " " " " square "		6.7"

Table V.

Without turbulence disk. Volume surface V_0 cm²	With turbulence disk I: Volume surface V_1 cm²	With turbulence disk I: Ratio of coefficients $\frac{\rho_1}{\rho_0} \left(\frac{V_1}{V_0}\right)^2$	With turbulence disk II: Volume surface V_2 cm²	With turbulence disk II: Ratio of coefficients $\frac{\rho_2}{\rho_0} \left(\frac{V_2}{V_0}\right)^2$	Mean % increase in coefficient due to turbulence
Brabbee's Pitot-Static Tube					
174.8	180.0	1.061	179.0	1.048	
263.6	271.0	1.057	271.9	1.057	5.4
368.9	377.2	1.046	378.5	1.053	
		1.055		1.053	
Rosenmüller's Pitot-Static Tube					
175.9	180.8	1.057	179.8	1.044	
265.2	270.3	1.038	270.7	1.042	4.2
371.7	375.9	1.023	379.8	1.046	
		1.039		1.044	
Baffle Plate with Round Edges					
210.7	223.1	1.118	223.5	1.124	
323.2	334.4	1.069	339.8	1.120	10.6
445.0	469.5	1.100	467.4	1.104	
		1.096		1.116	
Baffle Plate with Square Edges					
211.7	219.2	1.073	219.0	1.070	
326.3	336.7	1.064	335.7	1.060	6.7
444.3	459.8	1.072	457.1	1.060	
		1.070		1.063	

This phenomenon may be explained as follows. The turbulence effect is the resultant of the reactions on both test points of the Pitot-static tube. At the front opening the turbulence causes a decrease in the measured pressure, as compared with the true dynamic pressure, since the turbulent air in the middle flows obliquely toward the opening. Likewise the observations at the [illegible] test point show a diminution of the pressure due to the [illegible] condition, which diminution is partially caused in a manner simi-lar to that occurring in the oblique position of the instrument. The two effects may partially offset each other, so as apparently to diminish the effect of the turbulence. This is manifestly the case with Prandtl's small-bore, component, Pitot-static tube, in which said effect is the strongest, as it was intended to be in designing the instrument. With the baffle plates, on the contrary, the second effect is much the greater. The somewhat greater turbulence effect with Brabbée's Pitot-static tube is related to the fact that, in the oblique position, the difference measurements at first yield too high values. These differences in the effect of turbulence on Pitot-static tubes are not great and it should also be remembered that the whirling arm calibrations are made in air not entirely free from turbulence. In practice, therefore, with a very turbulent air stream, we can base our calculations on a probable increase of about 3% in the value of the pressure-velocity constant. We failed to establish that any turbulence effect depended on the velocity of flow, though such dependence probably exists to a small extent, since the degree of turbulence along with the magnitude of the disturbance depends on the velocity. This is apparently concealed by the unavoidable experimental inaccuracies.

Table VI.

Baffle plates compared with Prandtl's Pitot-static tube

β_s = pressure-velocity constant of baffle plate
β_p = " " " " Prandtl's Pitot-static tube
The numerals 0, 1, 2 = pressure-velocity constants by measurement without or with turbulence disks I or II.

Baffle plates with round edges								
Without turbulence disk			With turbulence disk I			With turbulence disk II		
Volume surface		Ratio of pressure-velocity constants	Volume surface		Ratio of pressure-velocity constants	Volume surface		Ratio of pressure-velocity constants
V_{p_0} cm²	V_{s_0} cm²	$\frac{\beta_{s_0}}{\beta_{p_0}} = \left(\frac{V_{s_0}}{V_{p_0}}\right)^2$	V_{p_1} cm²	V_{s_1} cm²	$\frac{\beta_{s_1}}{\beta_{p_1}} = \left(\frac{V_{s_1}}{V_{p_1}}\right)^2$	V_{p_2} cm²	V_{s_2} cm²	$\frac{\beta_{s_2}}{\beta_{p_2}} = \left(\frac{V_{s_2}}{V_{p_2}}\right)^2$
173.1	209.3	1.463	176.3	221.4	1.579	171.8	218.1	[illegible]
263.2	323.3	1.508	265.9	337.5	1.587	266.8	338.5	[illegible]
361.0	444.1	1.516	369.2	466.7	1.596	362.9	459.0	[illegible]
Mean ratio of pressure-velocity constants								
		1.496			1.587			[illegible]
Baffle plates with square edges								
173.1	211.1	1.488	176.3	220.3	1.568	171.8	[illegible]	[illegible]
263.2	326.6	1.540	265.9	337.4	1.613	266.8	[illegible]	[illegible]
361.0	443.4	1.510	369.2	458.4	1.543	362.9	[illegible]	[illegible]
Mean ratio of the coefficients								
		1.513			[illegible]			[illegible]

Table VII.

Round-edged baffle plates compared with Prandtl's Pitot-static tube.
(Symbols the same as in Table VI)

Without turbulence disk.

R mm	Small velocity: Dynamic pressure q_p mm water	Small velocity: Dynamic pressure q_s mm water	Small velocity: $\beta_s = \frac{q_s}{q_p}\beta_p$, $\beta_p = 1$	Medium velocity: Dynamic pressure q_p mm water	Medium velocity: Dynamic pressure q_s mm water	Medium velocity: $\beta_s = \frac{q_s}{q_p}\beta_p$, $\beta_p = 1$	Great velocity: Dynamic pressure q_p mm water	Great velocity: Dynamic pressure q_s mm water	Great velocity: $\beta_s = \frac{q_s}{q_p}\beta_p$, $\beta_p = 1$
140	2.31	3.71	1.605	5.35	8.95	1.672	10.09	16.78	1.662
135	2.39	3.68	1.540	5.44	8.86	1.627	10.23	16.34	1.597
130	2.38	3.59	1.508	5.50	8.52	1.549	10.37	16.03	1.547
120	2.39	3.44	1.438	5.56	8.14	1.480	10.43	15.32	1.469
110	2.40	3.38	1.406	5.59	8.06	1.441	10.48	15.30	1.460
100	2.44	3.38	1.385	5.62	8.13	1.446	10.55	15.20	1.441
85	2.43	3.34	1.374	5.65	8.16	1.444	10.62	15.26	1.436
70	2.44	3.41	1.397	5.65	8.16	1.444	10.62	15.40	1.450
50	2.43	3.41	1.403	5.63	8.12	1.443	10.67	15.40	1.443
35	2.40	3.44	1.433	5.64	8.12	1.440	10.70	15.42	1.443
0	2.29	3.48	1.518	5.63	8.21	1.458	10.68	15.42	1.441
		Mean value	1.419		Mean value	1.450		Mean value	1.448

Mean pressure-velocity constant $\beta_s = 1.439$

Table VIII.

Round-edged baffle plates compared with Prandtl's Pitot-static tube.
(Symbols the same as in Table VI.)

With turbulence disk I.

R	Small velocity			Medium velocity			Great velocity		
	Dynamic pressure			Dynamic pressure			Dynamic pressure		
	q_p	q_s	$\beta_s = \frac{q_s}{q_p} \beta_p$	q_p	q_s	$\beta_s = \frac{q_s}{q_p} \beta_p$	q_p	q_s	$\beta_s = \frac{q_s}{q_p} \beta_p$
mm	mm water	mm water	$\beta_p = 1$	mm water	mm water	$\beta_p = 1$	mm water	mm water	$\beta_p = 1$
140	2.07	3.68	1.777	4.80	8.61	1.794	10.06	16.81	1.672
135	2.25	3.70	1.645	5.21	8.68	1.667	9.81	16.28	1.660
130	2.40	3.82	1.597	5.50	8.86	1.612	10.25	16.49	1.607
120	2.53	3.99	1.577	5.71	9.20	1.612	10.90	17.16	1.574
110	2.66	4.04	1.519	5.99	9.39	1.568	11.24	17.40	1.546
100	2.62	4.02	1.535	5.95	9.53	1.601	11.34	18.05	1.591
85	2.62	4.05	1.546	5.89	9.60	1.630	11.50	17.91	1.557
70	2.66	4.19	1.576	6.08	9.70	1.596	11.50	18.36	1.559
50	2.64	4.14	1.568	6.09	9.67	1.588	11.59	18.37	1.584
35	2.72	4.25	1.563	6.12	9.66	1.579	11.39	18.23	1.602
0	2.65	4.20	1.602	6.08	9.73	1.601	11.40	18.39	1.612
		Mean value	1.561		Mean value	1.598		Mean value	1.578

Mean pressure-velocity constant $\beta_s = 1.579$

Table IX.

Round-edged baffle plates compared with Prandtl's Pitot-static tube.
(Symbols the same as in Table VI)

With turbulence disk II.

R	Small velocity: Dynamic pressure q_p	q_s	$\beta_s = \frac{q_s}{q_p}\beta_p$	Medium velocity: Dynamic pressure q_p	q_s	$\beta_s = \frac{q_s}{q_p}\beta_p$	Great velocity: Dynamic pressure q_p	q_s	$\beta_s = \frac{q_s}{q_p}\beta_p$
mm	mm water	mm water	$\beta_p = 1$	mm water	mm water	$\beta_p = 1$	mm water	mm water	$\beta_p = 1$
140	2.06	3.48	1.690	4.77	8.45	1.772	8.84	15.30	1.732
135	2.23	3.51	1.574	5.18	8.55	1.651	9.53	15.60	1.638
130	2.43	3.61	1.485	5.47	8.74	1.598	10.00	16.10	1.610
120	2.39	3.78	1.582	5.76	8.97	1.558	10.56	16.52	1.566
110	2.43	3.81	1.568	5.86	9.18	1.567	10.94	16.97	1.549
100	2.45	3.86	1.574	6.04	9.46	1.567	11.12	17.28	1.553
85	2.46	3.96	1.608	6.16	9.84	1.597	11.35	17.50	1.543
70	2.46	3.97	1.613	6.18	9.63	1.559	11.28	17.63	1.564
50	2.45	3.96	1.616	6.20	9.68	1.562	11.50	17.87	1.553
35	2.45	4.02	1.643	6.21	9.80	1.579	11.59	17.89	1.544
0	2.45	4.10	1.673	6.20	9.73	1.570	11.50	18.07	1.570
		Mean value	1.610		Mean value	1.570		Mean value	1.555

Mean pressure-velocity constant $\beta_s = 1.578$

In Table V, the pressure-velocity constants computed for the baffle plates are too favorable. It was found that, even in the undisturbed flow, the effect of the turbulence due to the friction of the walls becomes noticeable in the boundary layer by the higher readings of the baffle plate and that the volume surfaces for this flow are accordingly too large. If, in Table VI, we compare the volume surfaces of the baffle plates for the undisturbed flow with the corresponding volume surfaces of Prandtl's Pitot-static tube, in which the turbulence effect is relatively small, we obtain, for the smooth flow, as the mean coefficient of the baffle plates, 1.496 against 1.433 or 1.513 against 1.448 of the whirling-arm calibration. If we now compare the mean dynamic pressure of the Pitot-static tube and the round-edged baffle plate for the individual rings (Tables VII-IX), the effect of the turbulent marginal layer is noticeable. For the undisturbed flow, it reaches to about r = 130 mm. With exclusion of the marginal values, the mean pressure-velocity constant of the round-edged baffle plate is 1.439, which agrees very well with the mean calibration value 1.433 of the whirling-arm experiments. The elevation of the pressure-velocity constant in the marginal layer, is, however, not due alone to the turbulent condition of the air, but also to the proximity of the wall, which similarly affects the pressure readings of the baffle plate. This is due to the fact that the pressure-velocity constants for the radii r = 130-140 in Table VII are considerably greater than what would correspond to the turbulence effect according to Tables VIII and IX for the turbulent flow and also to the fact that, for the turbulent flow, the pressure-velocity constants for both these radii likewise far exceed the mean value for the central portion of the stream (r = 120 - 0). In order to separate the effect of the turbulence from that of the wall, we would have to improve the volume curves for the marginal layer with the aid of the pressure-velocity constant for the central portion of the cross-section and thus obtain new volume surfaces. Since, however, the value of the baffle plates is now very small, we have not made these calculations.

VII.- WHIRLING-ARM CALIBRATIONS.

The pressure difference p_1 measured with the Pitot-static tube is proportional to the dynamic pressure q of the flow velocity. The proportionality factor is therefore $\rho = \frac{p_1}{q}$, where $q = \frac{\gamma v^2}{2g}$ represents the dynamic pressure of the flow. Its determination, i.e., the calibration of the instrument, was accomplished with the whirling-arm in the manner first described by Recknagel ("Ueber Luftwiderstand," Annalen der Physik und Chemie, Vol. X, 1880). The method consists in causing the instrument to move through the air at a velocity which is calculated from the number of revolutions per second and the radius of the circle described by the instrument on the whirling-arm and in simultaneously observing the pressure difference between the nose of the instrument and the slot. In this method, however, there is one disturbing factor, namely, the air swirl created by the whirling-arm, so that the relative velocity v of the Pitot-static tube, on which the pressure at its nose depends, is less than the speed u of the whirling-arm. Recknagel attempted to determine the velocity of the air swirl by comparing the pressure measurements during the first revolutions of the apparatus (before the creation of any appreciable swirl) with subsequent pressure measurements. No great accuracy could be obtained in this manner, since, even if a uniform speed were attained during the first revolution, the inertia of the micromanometer prevented any immediate reading. Another much-employed method for determining the swirl velocity consisted in mounting a sensitive anemometer near the path of the Pitot-static tube (Stack, "Ueber Mitwindbestimmungen bei Anemometer-Prüfungen," Annalen der Hydrographie und maritimen Meteorologie, 1904, or Technical Reports of the Advisory Committee for Aeronautics (British), No. 71, December, 1912). This method, however, gives only temporary mean values which may easily be too large, on account of the inertia of the anemometer. The following method, also invented by Recknagel, is more reliable and convenient. In addition to the pressure difference p_1 between the slot and nose, the pressure at the nose is also measured by a second manometer, whereby it is assumed that the static pressure is uniform throughout the experiment room, which is the case, excepting for the vortex regions behind the whirling arm and the Pitot-static tube. The direct measurement of the pressure at the nose is, however, impossible, on account of the centrifugal force p_c in the pressure-transmitting tube on the whirling-arm. On the contrary, the second manometer measures the difference p_2 between the centrifugal force and the pressure at the nose. Thus

$$p_2 = p_c - \frac{\gamma v^2}{2g}$$

If ω denotes the angular speed of the whirling-arm, u its peripheral speed, and z the number of revolutions in the time T, the centrifugal force, on the assumption that the air is not hereby compressed, is

$$p_c = \frac{\gamma}{g} \omega^2 \int_{\rho=r}^{\rho=R} \rho \, d\rho = \frac{\gamma}{2g} \omega^2 (R^2 - r^2) = \frac{\gamma}{2g} u^2 \left(1 - \frac{r^2}{R^2}\right)$$

or (if, instead of u, the observed values of z and T are introduced, i.e., $u = 2 \pi R \times \frac{Z}{T}$)

$$p_c = \frac{2 \pi^2 R^2}{g} \left(1 - \frac{r^2}{R^2}\right) \gamma \left(\frac{Z}{T}\right)^2$$

(The ratio r : R is usually very small, here about 6 : 274, so that, in comparison with 1, its square may be disregarded. Here the error is about 0.05%.) Here R is the radius of the circle whose circumference is the path of the Pitot-static tube and r is the radius of the chamber, on the whirling-arm axis, from which the pressure is transmitted to the manometer. The pressure exerted by the centrifugal force is therefore equal to that of the absolute speed and the relative dynamic pressure is therefore

$$\frac{\gamma v^2}{2g} = p_c - p_2 .$$

whereby the pressure-velocity constant becomes

$$\beta = \frac{p_1}{p_c - p_2}$$

In the whirling-arm mechanism employed, the vertical shaft is driven by an electric motor, through a belt, chain and worm gear. The maximum radius, at which the instrument can be fastened, is about 2.75 m and the maximum absolute speed, thus attained by the smooth running of the whirling-arm, is about 17 m/s. The arm has an elliptical cross-section 40 x 140 mm, in order to penetrate the air with as little disturbance as possible and keep the swirl velocity as low as possible. The swirl velocity is here 3.5-4% of the absolute speed of the arm. By a special device the instrument is held about 0.5 m in front of and about 0.35 m above the arm, so that there would seem to be no possibility of the readings of the instrument being affected by any reaction of the arm. The instrument is guyed to the arm with a steel wire of 2 mm diameter, so that the radius cannot be affected by the centrifugal force during the measurement. The reading of the pressure at the axle is made under a water-sealed rotating bell (Fig. 50).

The calculation of the pressure exerted by the centrifugal force requires an accurate determination of the number of revolutions during the observation period. This is done electrically, by making a mark for each revolution on the moving strip of paper in a chronograph. The time-marks at one-second intervals are made by the main clock of the laboratory. The chronograph is driven by the worm-gear shaft, the paper band being carried along by friction. The paper band was of such length that about 40 revolutions could be recorded. The spaces were of uniform length and furnished the scale for the partial revolutions in a given period of time. The uniform length of the spaces between the time-marks rendered it possible to test the uniformity of the revolution speed. Due to the resistance in the long pipes, the manometer for the difference measurements was slow to respond to disturbances in the state of equilibrium of the whirling-arm. In order to obtain an experimental basis for judging its worth, the manometer deflection was observed for a time after the termination of the chronograph strip and the results of the experiment were used only when the manometer readings remained constant.

The air density was determined from the temperature and barometer reading. The latter had to be corrected for the vapor tension of the air (Kohlrausch, "Lehrbuch der praktischen Physik," Leipzig, 1910, Chapters 13 and 47). Damp air can be up to about 1% lighter than dry air. The moisture content of the air was determined by an Assmann aspiration psychrometer. The results are given in Tables X-XV, but in detail only for the three principal types of the Pitot-static tube and the two baffle plates. The pressure-velocity constant for all three Pitot-static tubes is practically 1 and independent of the velocity, which renders them suitable for the direct measurement of the static pressure. Where there appears to be a slight decrease in the pressure-velocity constant with decreasing velocity, especially with the baffle plates, this may be due to a less degree of turbulence in the air at low velocities. The mean pressure-velocity constant of 1.44 for both baffle plates agrees very closely with that (1.45) obtained by the "Prüfungsanstalt für Heizung und Lüftung."

VIII. - SUMMARY

In connection with the pressure distribution on a solid of revolution, we have explained the functioning of Pitot-static tubes, with special attention to the one designed by Prandtl. We have shown that a new form, finally adopted by Prandtl, largely satisfied the requirements of a practical instrument. Its pressure-velocity constant was found by the whirling-arm calibration to be approximately 1. Hence the Pitot-static tube is adapted for measuring both velocity and static pressure. It gives accurate velocity measurements when inclined up to $\pm 15^\circ$. In a very turbulent flow, it gives the velocity about 4% too high.

We have described special forms for making measurements in air containing dust and in the moist air of mines. By reducing the bore in the nose, the instrument was adapted for use as a "component" tube in a range of about $\pm 30^\circ$ with an error of less than 2%, while showing the axial velocity component in the axial position in an oblique current.

For comparison, we tested a Brabbée and a Rosenmuller

Pitot-static tube, as also a round-edged and a square-edged baffle plate. Both tubes had the same pressure-velocity constant and about the same sensitivity to turbulence. The sensitivity of both tubes to inclination was greater than for Prandtl's Pitot-static tube. The pressure-velocity constant of 1.37 for baffle plates, as given by Recknagel, was found to be too small. It was 1.44 and increased about 10% in a very turbulent current or in the vicinity of the walls of the pipe.

All three Pitot-static tubes are of about equal merit, as regards their facility of accurate reproduction, their pressure-velocity constant and their sensitivity to turbulence. Prandtl's tube surpasses both the others in its smaller degree of sensitivity in the oblique position. Rosenmuller's tube, in its present form, is not convenient for practical use.

Baffle plates should be discarded in favor of Pitot-static tubes, on account of the variable value of the pressure-velocity constant of the former.

Table X.

Prandtl's Pitot-static tube - normal form

Barometer B mm Hg	Psychrometer t °C	Psychrometer t' °C	Corrected barometer reading B_o mm Hg	Air density γ kg/m^3	Revolutions of whirling-arm Z	Time T s	Centrifugal force p_c kg/m^2	Difference measurement p_1 kg/m^2	Pressure at nose p_2 kg/m^2	Dynamic pressure of the relative speed $\frac{\gamma v^2}{2g}=p_c-p_2$ kg/m^2	Relative speed v m/s	Pressure velocity constant $\beta=\frac{p_1}{\frac{\gamma v^2}{2g}}$
744.6	16.0	12.3	741.3	1.191	40.056	45	14.202	13.19	1.046	13.156	14.70	1.002
744.6	15.8	12.2	741.3	1.192	40.516	49	12.267	11.41	0.906	11.361	13.68	1.003
744.6	15.8	12.1	741.3	1.192	39.234	56	8.905	8.36	0.625	8.280	11.61	1.010
744.6	15.6	12.1	741.3	1.193	39.933	67	6.374	5.984	0.423	5.951	9.64	1.005
744.6	15.6	12.0	741.3	1.193	38.297	80	4.113	3.838	0.282	3.831	7.93	1.001
744.6	15.5	12.0	741.3	1.194	39.449	89	3.529	3.295	0.246	3.283	7.35	1.003
744.6	15.4	11.8	741.4	1.194	38.559	108	2.289	2.129	0.159	2.130	5.91	1.000
748.0	16.1	12.6	744.6	1.196	36.322	131	1.273	1.177	0.094	1.179	4.37	1.000
											Mean value	1.003

Table XI.

Prandtl's Pitot-static tube.

Old form		Narrow bore		Wide bore		Rounded slot	
Speed v m/s	Pressure velocity constant β	Speed v m/s	Pressure velocity constant β	Speed v m/s	Pressure velocity constant β	Speed v m/s	Pressure velocity constant β
12.39	1.015	16.45	1.009	16.27	1.001	16.00	1.002
11.53	1.005	15.21	1.003	14.50	1.003	15.03	1.002
10.44	1.017	12.12	1.005	12.97	1.003	13.09	1.007
9.07	1.016	11.01	0.998	11.01	1.004	11.75	0.999
8.42	1.013	10.61	1.001	8.38	0.997	10.05	1.002
7.40	1.020	9.05	1.000	8.25	0.998	8.40	0.996
5.76	1.019	8.36	1.004	7.26	0.996	7.62	1.000
4.98	1.004	7.42	1.003	5.82	0.995	6.47	0.990
3.50	1.007	6.12	1.008	4.21	0.993	4.00	0.974
		4.68	0.993				
Mean value 1.013		Mean value 1.002		Mean value 0.999		Mean value 0.997	

Table XII.

Brabbee's Pitot-static tube.

Barometer	Psychrometer		Corrected barometer reading	Air density	Revolutions of whirling-arm	Time	Centrifugal force	Difference measurement	Pressure at nose	Dynamic pressure of the relative speed	Relative speed	Pressure velocity constant
B	t	t'	B	γ	Z	T	p_c	p_1	p_2	$\frac{\gamma v^2}{2g} = p_c - p_2$	v	$\beta = \frac{p_1}{\frac{\gamma v^2}{2g}}$
mm Hg	°C	°C	mm Hg	kg/m³		s	kg/m²	kg/m²	kg/m²	kg/m²	m/s	
744.7	15.6	11.8	741.5	1.193	38.943	40	17.04	15.72	1.273	15.767	16.10	0.997
744.7	15.8	12.0	741.5	1.193	39.596	44	14.56	13.51	1.060	13.500	14.90	1.001
744.7	16.7	12.5	741.4	1.189	37.805	48	11.11	10.34	0.801	10.309	13.03	1.003
744.7	17.0	12.7	741.4	1.188	39.003	61	7.32	6.87	0.476	6.844	10.62	1.004
744.4	17.0	12.8	741.0	1.187	38.741	76	4.65	4.324	0.305	4.345	8.45	0.995
744.4	17.0	12.8	741.0	1.187	39.441	93	3.22	3.015	0.217	3.003	7.02	1.004
744.4	17.0	12.9	741.0	1.187	40.275	122	1.95	1.817	0.134	1.816	5.48	1.000
744.4	17.0	12.9	741.0	1.187	39.194	201	0.78	0.727	0.058	0.722	3.44	1.007
											Mean value	1.001

Table XIII.

Rosenmuller's Pitot-static tube.

Barometer	Psychrometer		Corrected barometer reading	Air density	Revolutions of whirling-arm	Time	Centrifugal force	Difference measurement	Pressure at nose	Dynamic pressure of the relative speed	Relative speed	Pressure velocity constant
B	t	t'	B	γ	Z	T	p_c	p_1	p_2	$\frac{\gamma v^2}{2g}=p_c-p_2$	v	$\beta=\frac{p_1}{\frac{\gamma v^2}{2g}}$
mm Hg	°C	°C	mm Hg	kg/m³		s	kg/m²	kg/m²	kg/m²	kg/m²	m/s	
741.2	14.2	10.0	738.5	1.202	40.215	41	17.233	16.11	1.113	16.120	16.22	0.999
741.2	14.2	10.0	738.5	1.202	36.868	42	13.800	12.92	0.889	12.911	14.51	1.001
741.2	14.2	10.1	738.5	1.202	40.595	50	11.824	11.01	0.749	11.075	13.43	0.994
741.2	14.2	10.1	738.5	1.202	40.972	56	9.591	8.89	0.615	8.976	12.09	0.990
741.2	14.2	10.2	738.5	1.202	40.480	67	6.539	6.05	0.410	6.129	10.00	0.985
741.2	14.3	10.2	738.5	1.202	39.539	77	4.743	4.413	0.294	4.449	8.52	0.992
741.2	14.3	10.2	738.5	1.201	39.532	84	3.967	3.709	0.249	3.718	7.78	0.998
741.2	14.4	10.3	738.5	1.201	40.663	100	2.958	2.757	0.180	2.778	6.73	0.992
741.2	14.4	10.3	738.5	1.201	39.711	110	2.332	2.167	0.137	2.195	5.98	0.987
741.2	14.5	10.3	738.5	1.201	39.486	132	1.601	1.490	0.084	1.517	5.06	0.982
											Mean value	0.992

Table [illegible]

Round-edged baffle plate

Barometer B mm Hg	Psychrometer t °C	Psychrometer t' °C	Corrected barometer reading B mm Hg	Air density γ kg/m³	Revolutions of whirling-arm Z	Time T s	Centrifugal force p_c kg/m²	Difference measurement p_1 kg/m²	Pressure at nose p_2 kg/m²	Dynamic pressure of the relative speed $\frac{\gamma v^2}{2g}=p_c-p_2$ kg/m²	Relative speed v m/s	Pressure velocity constant $\beta=\frac{p_1}{\frac{\gamma v^2}{2g}}$
756.9	17.2	11.5	754.2	1.207	39.673	41	16.896	22.72	1.284	15.612	15.92	1.457
756.9	17.2	11.5	754.2	1.207	39.740	45	14.436	19.19	1.047	13.389	14.76	1.433
756.9	17.2	11.5	754.2	1.207	40.286	51	11.249	15.03	0.827	10.422	13.01	1.442
756.9	17.3	11.7	754.1	1.207	39.457	57	8.647	11.61	0.638	8.009	11.40	1.450
756.9	17.3	11.7	754.1	1.207	40.811	66	6.918	9.21	0.529	6.389	10.18	1.442
756.9	17.4	11.8	754.1	1.206	40.276	83	4.261	5.59	0.328	3.933	8.00	1.422
756.9	17.4	12.0	754.0	1.205	38.470	88	3.440	4.595	0.256	3.184	7.19	1.443
756.9	17.4	12.0	754.0	1.205	40.396	101	2.880	3.850	0.215	2.665	6.57	1.445
756.9	17.5	12.2	753.9	1.205	39.350	120	1.935	2.537	0.137	1.798	5.40	1.411
756.9	17.5	12.2	753.9	1.205	40.263	152	1.263	1.635	0.063	1.130	4.38	1.386
											Mean value	1.433

Table XV.

Square-edged baffle plate.

Barometer B mm Hg	Psychrometer t °C	Psychrometer t' °C	Corrected barometer reading B mm Hg	Air density γ kg/m³	Revolutions of whirling-arm Z	Time T s	Centrifugal force p_c kg/m²	Difference measurements p_1 kg/m²	Pressure at nose p_2 kg/m²	Dynamic pressure of the relative speed $\frac{\gamma v^2}{2g}=p_c-p_2$ kg/m²	Relative speed v m/s	Pressure velocity constant $\beta=\frac{p_1}{\frac{\gamma v^2}{2g}}$
751.8	16.9	12.2	748.7	1.205	40.562	42	16.759	22.82	1.264	15.495	16.36	1.473
751.8	17.0	12.3	748.7	1.204	40.658	47	13.435	18.25	1.022	12.413	14.23	1.470
751.8	17.0	12.3	748.7	1.204	40.016	56	9.231	12.59	0.662	8.569	11.82	1.469
751.8	17.2	12.4	748.7	1.204	40.609	67	6.660	9.06	0.467	6.193	10.04	1.463
751.8	17.3	12.5	748.6	1.203	40.610	90	3.652	4.97	0.259	3.393	7.44	1.465
751.8	18.2	12.9	748.6	1.200	40.392	95	3.335	4.377	0.214	3.081	7.02	1.449
751.8	18.2	12.9	748.6	1.200	39.407	104	2.569	3.490	0.165	2.404	6.26	1.452
751.8	18.4	13.2	748.5	1.199	39.411	118	1.995	2.671	0.122	1.873	5.54	[illegible]
751.8	18.4	13.2	748.5	1.199	40.170	143	1.411	1.869	0.089	1.322	4.65	[illegible]
751.8	18.7	13.6	748.4	1.198	39.700	180	0.869	1.119	0.068	0.801	3.62	[illegible]
											Mean value	[illegible]

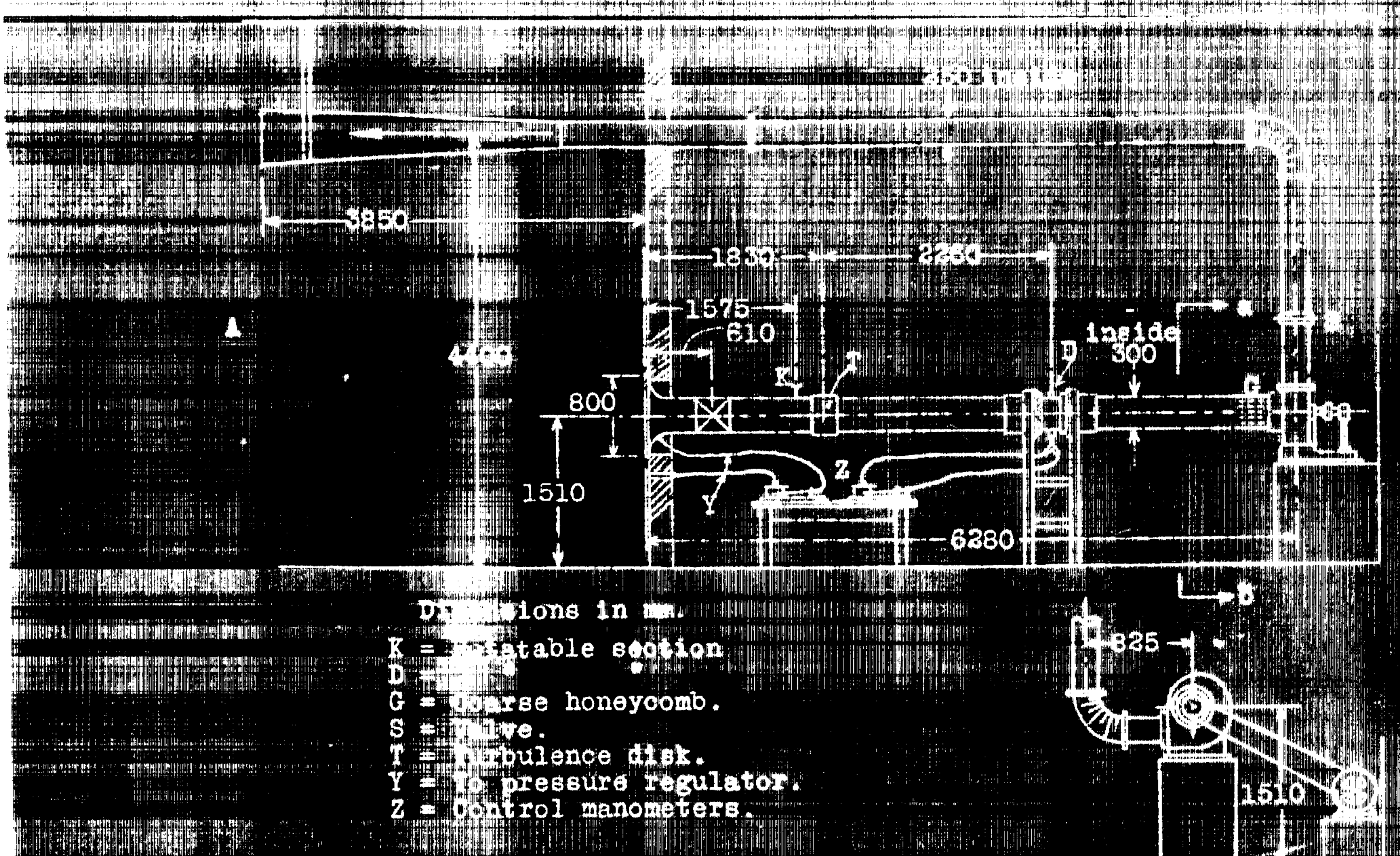

Section at a-b

Figs.1,2. Arrangement for experiment.

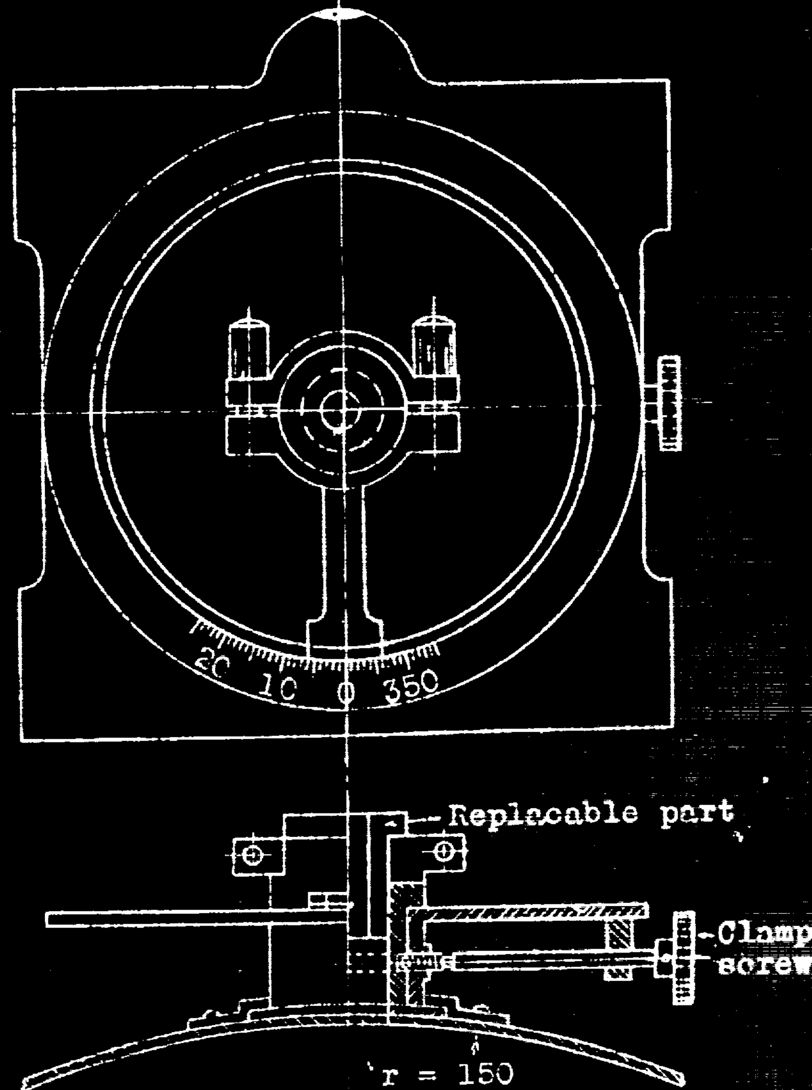

Figs. 3,4 Rotatable section for mounting the Pitot-static tube

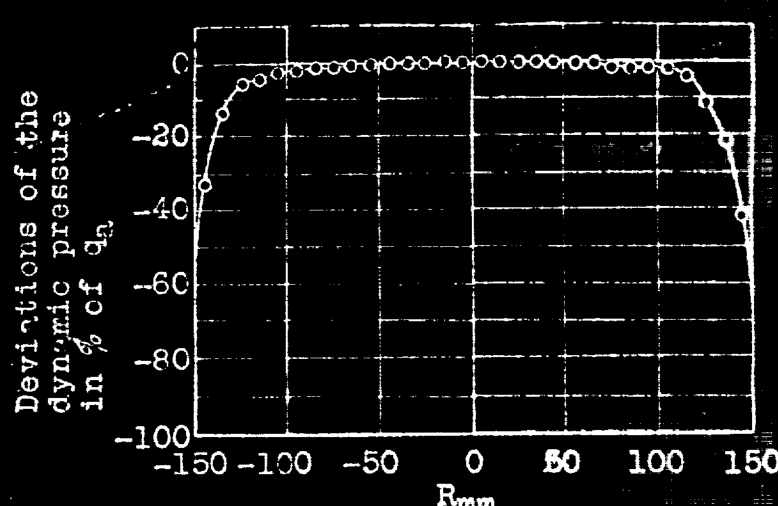

Fig.5 Distribution of the dynamic pressure on the experimental cross-section, q_n = 6.07 mm W. S.

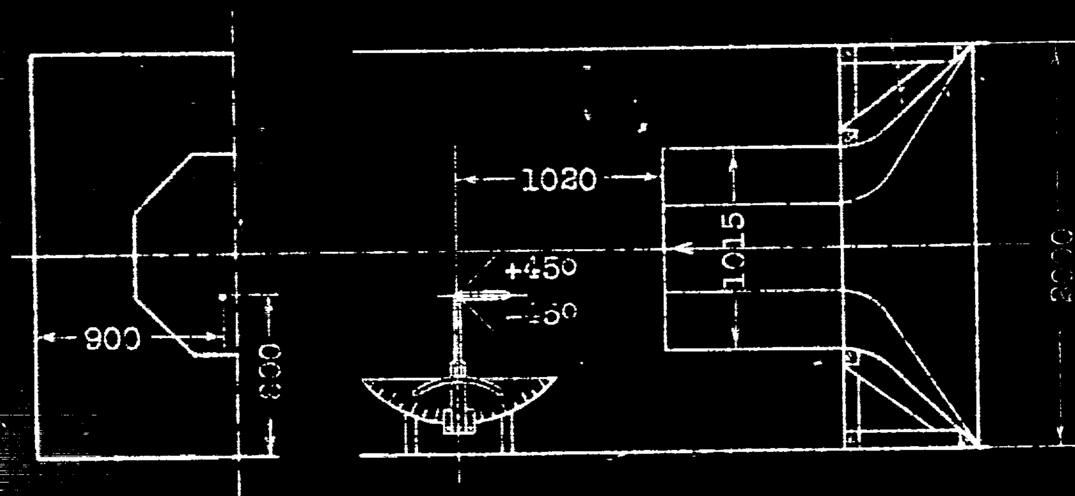

Figs. 6,7 Arrangement for testing the pressure course by turning about the transvers axis.

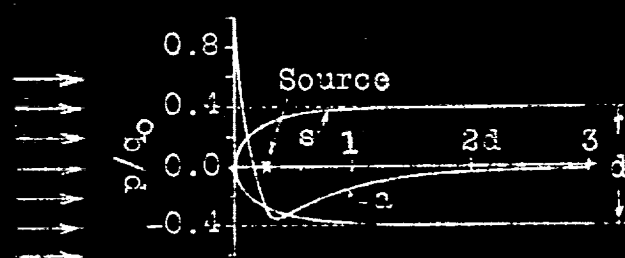

Fig. 8 Pressure distribution on a conoid.

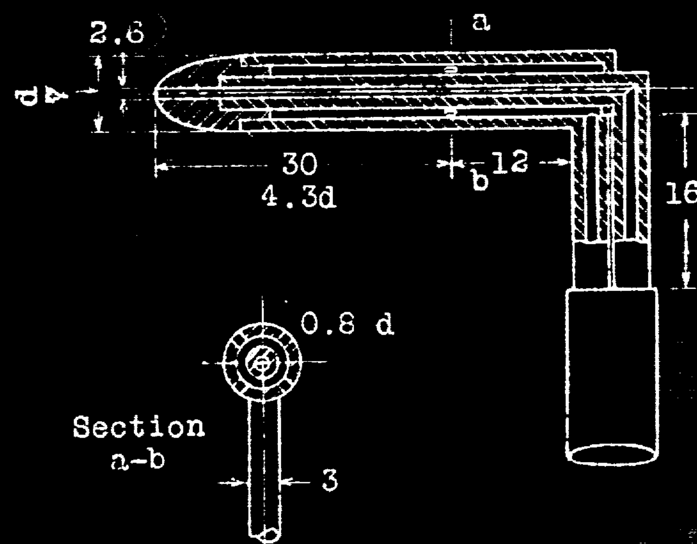

Figs. 9,10 Prandtl's Pitot-static tube. Old form

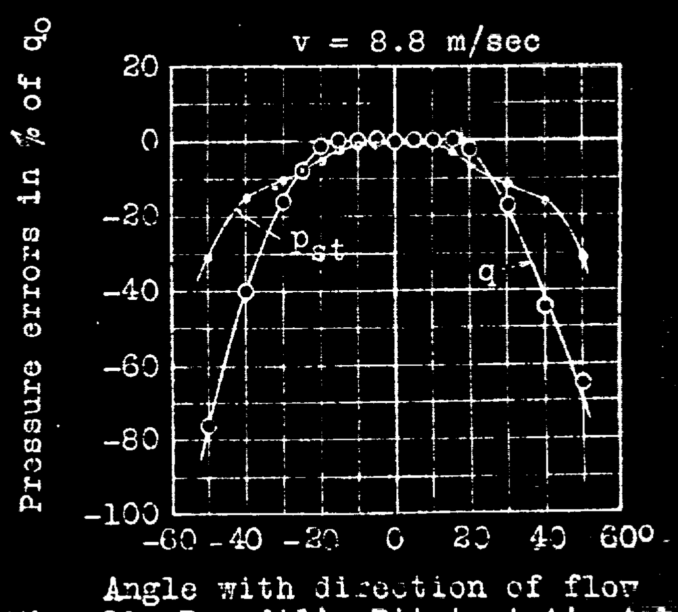

Fig. 11 Prandtl's Pitot-static tube. Old form.(Turning about the spindle).

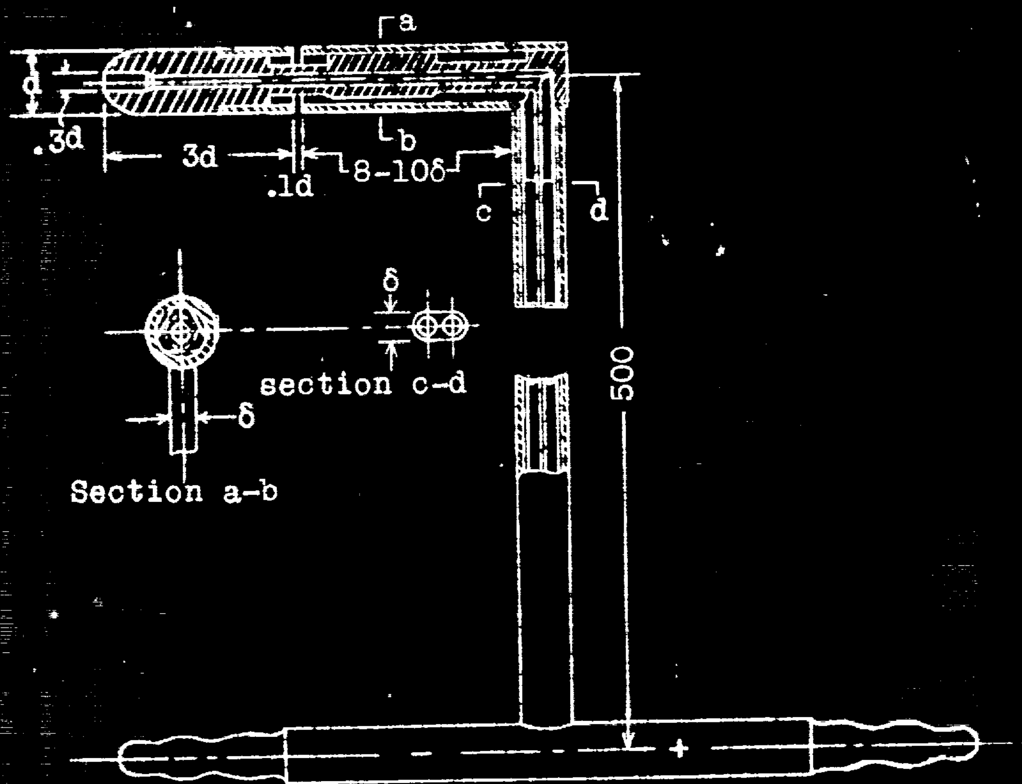

Figs.12,13,14. Prandtl's pitot-static tube. (New form)

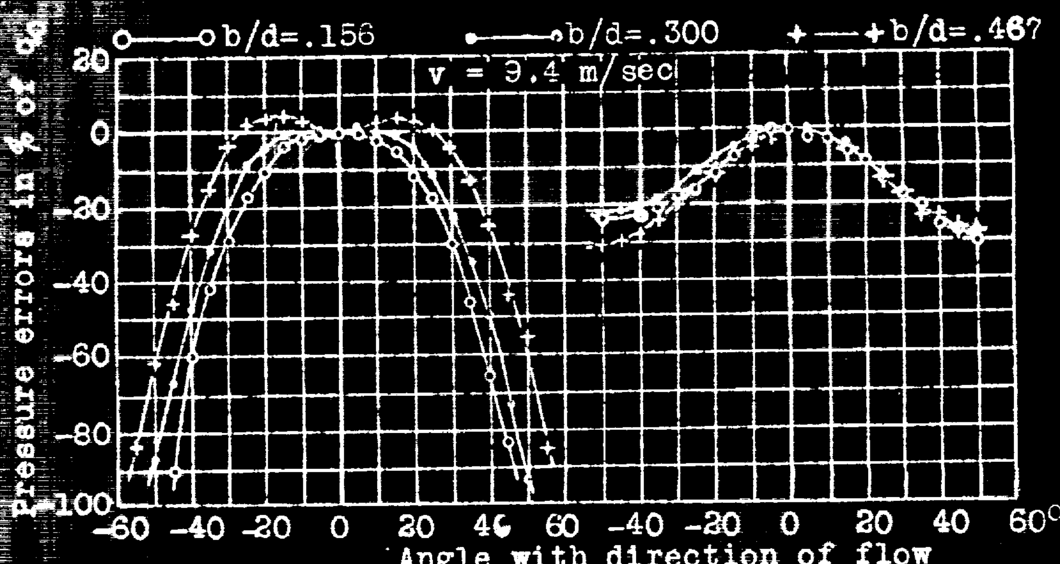

Figs.15,16. Effect of bore on dynamic and static pressure.

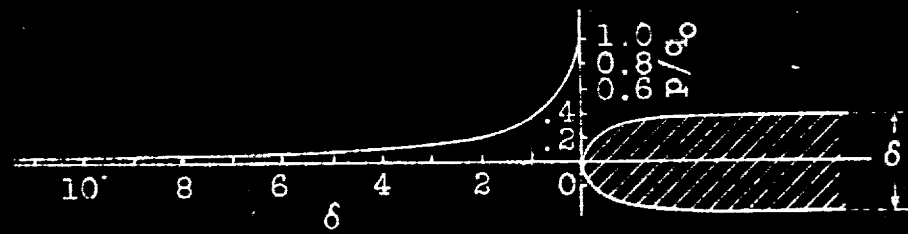

Fig. 17 Damming effect in front of a symmetrical conoid.

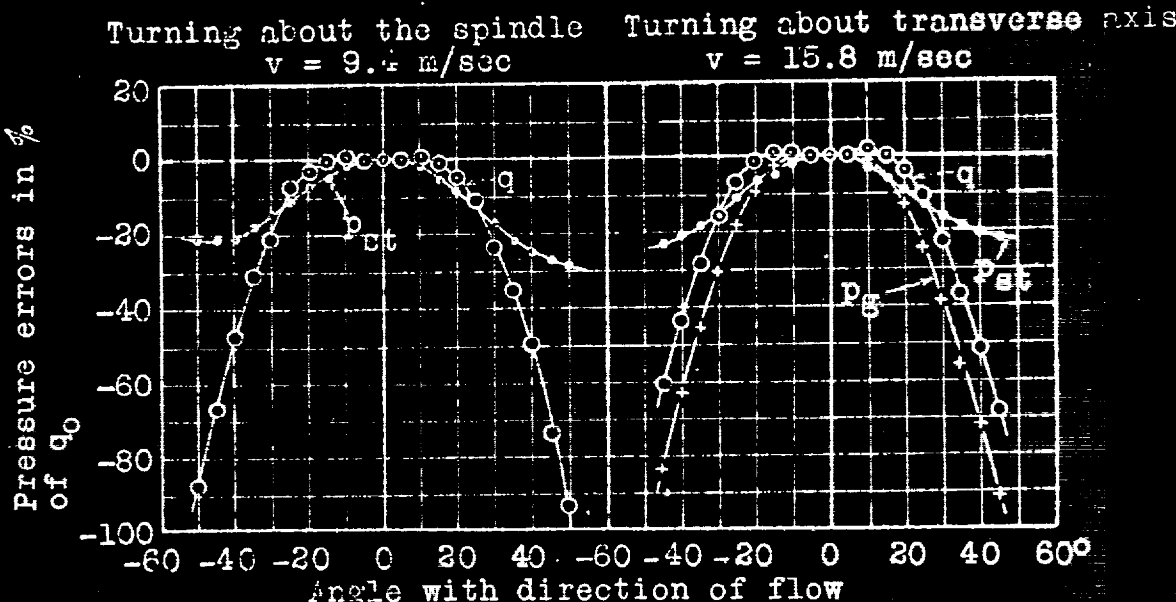

Figs. 18,19 Prandtl's Pitot-static tube. New form

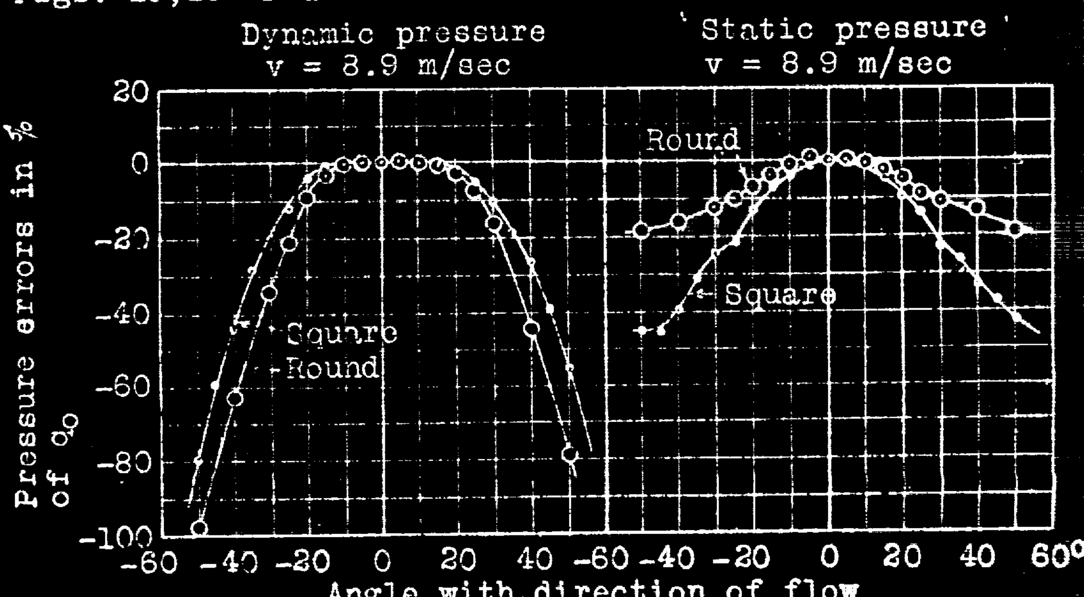

Figs. 20,21 Effect of shape of slot edges.

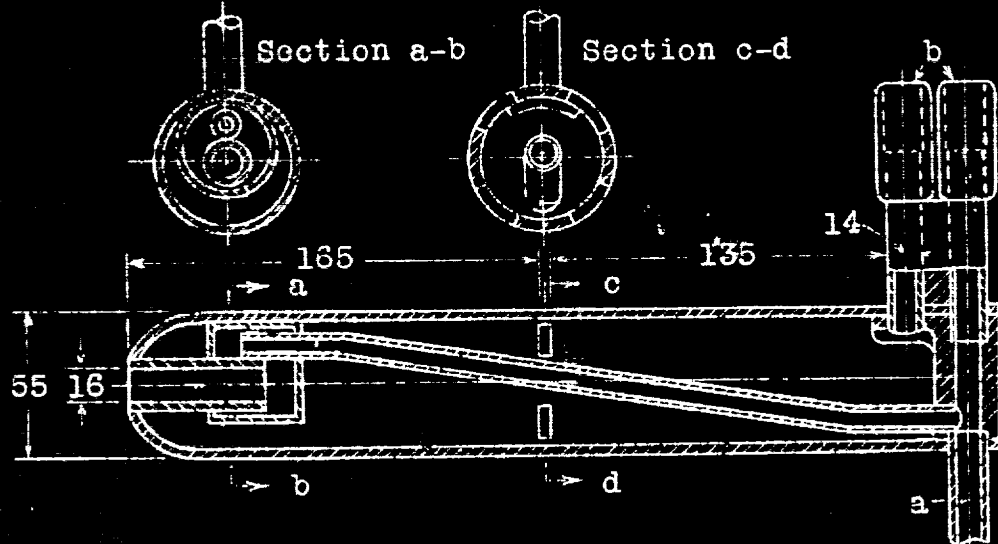

Figs. 22,23,24 Instrument for use in mines

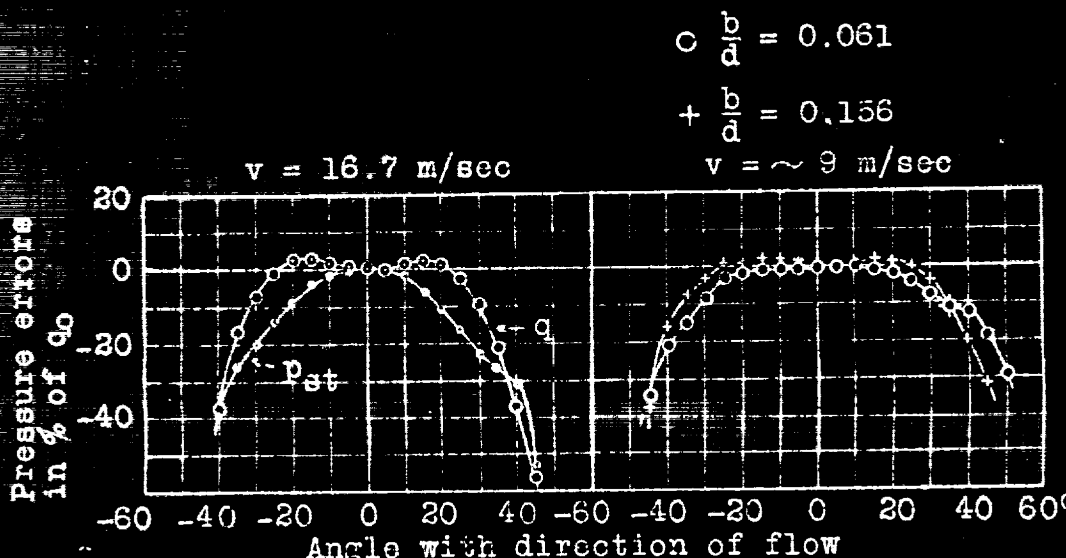

Fig. 25 Mine instrument. Turning about spindle axis.

Fig. 26 Component form of Prandtl's Pitot-static tube.

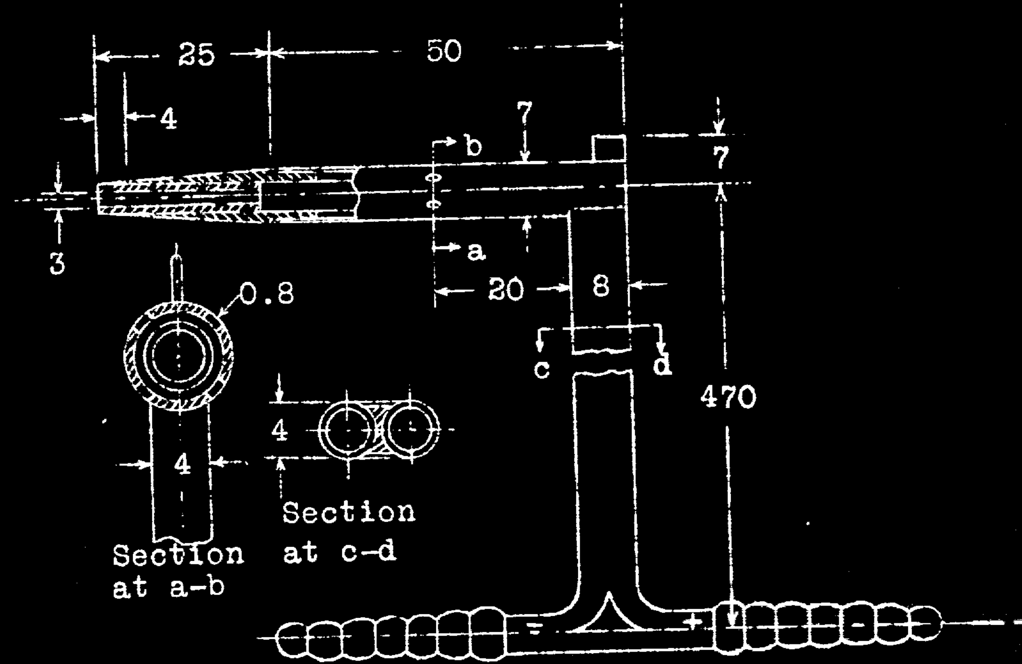

Figs.27,28 & 29 Brabbée's pitot-static tube.

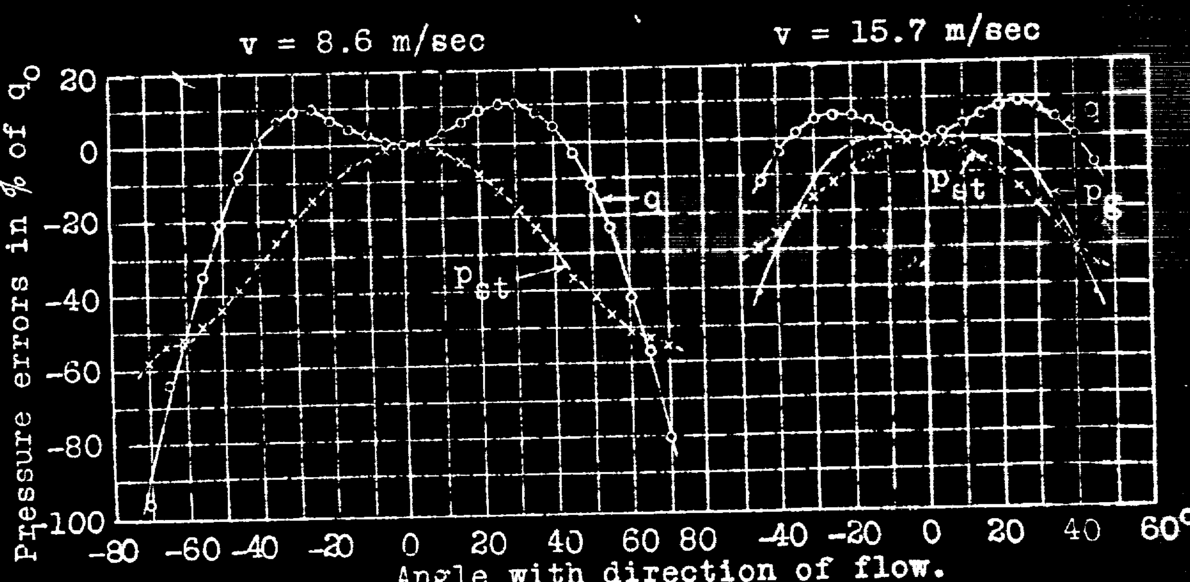

Fig.30 Brabbée's pitot-static tube, turning about spindle axis.

Fig.31 Brabbée's pitot-static tube, turning about transverse axis.

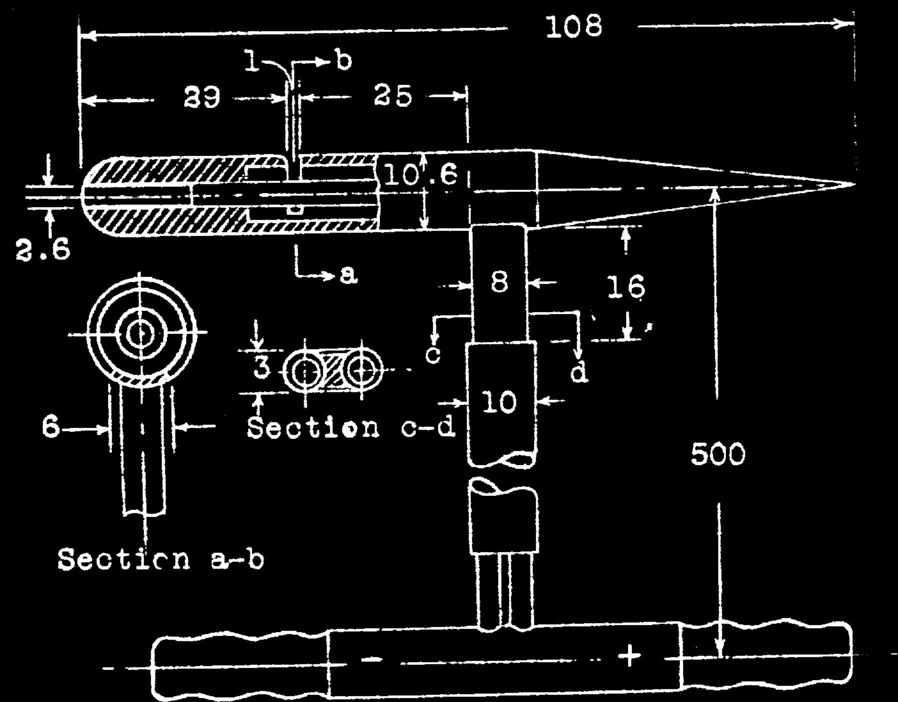

Figs.32,33,34. Rosenmüller's pitot-static tube.

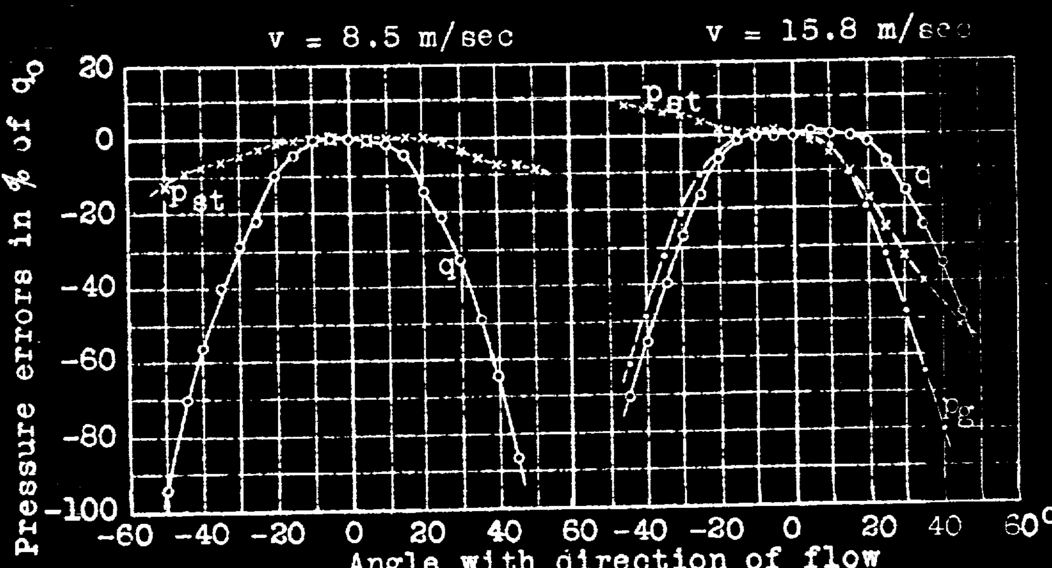

Fig.35 Rosenmüller's pitot-static tube. Turning about the spindle axis.

Fig.36 Rosenmüller's pitot-static tube. Turning about the transverse axis.

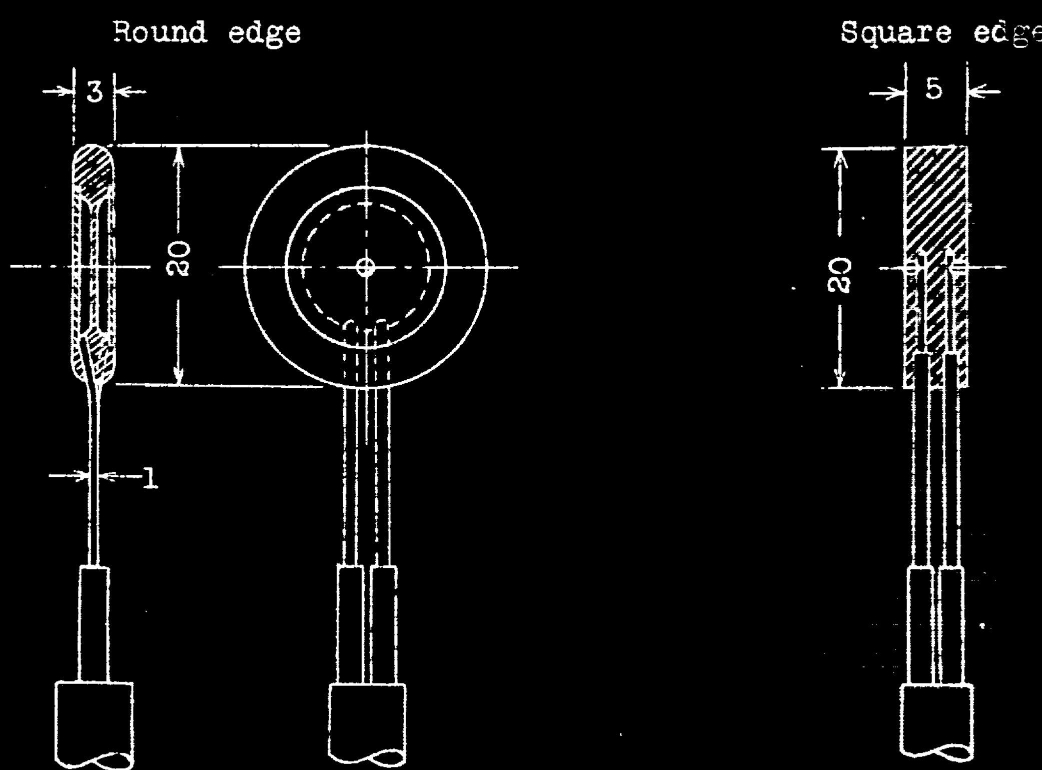

Figs.37,38,39. Baffle plates.

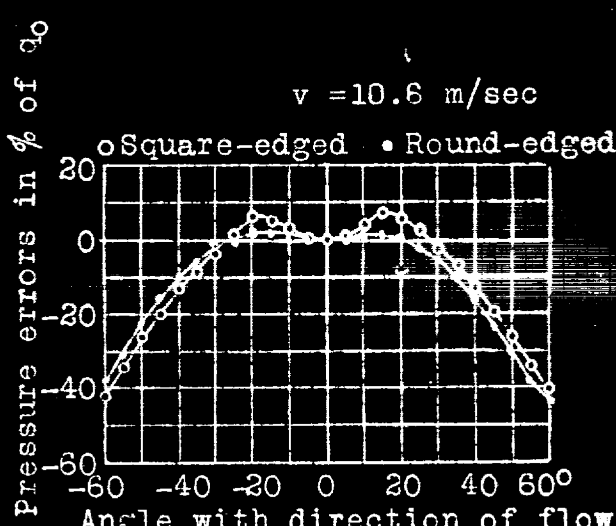

Fig.40 Turning about spindel axis.

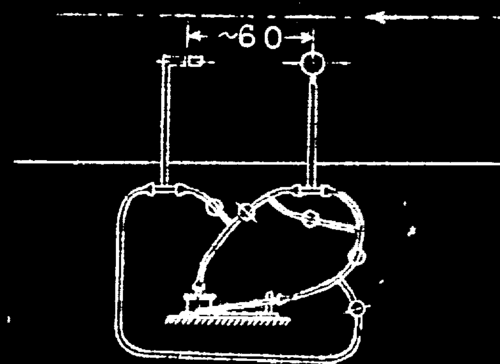

Fig.41 Comparison of pressure reading of a transverse baffle plate with the reading of the slot of a pitot-static tube.

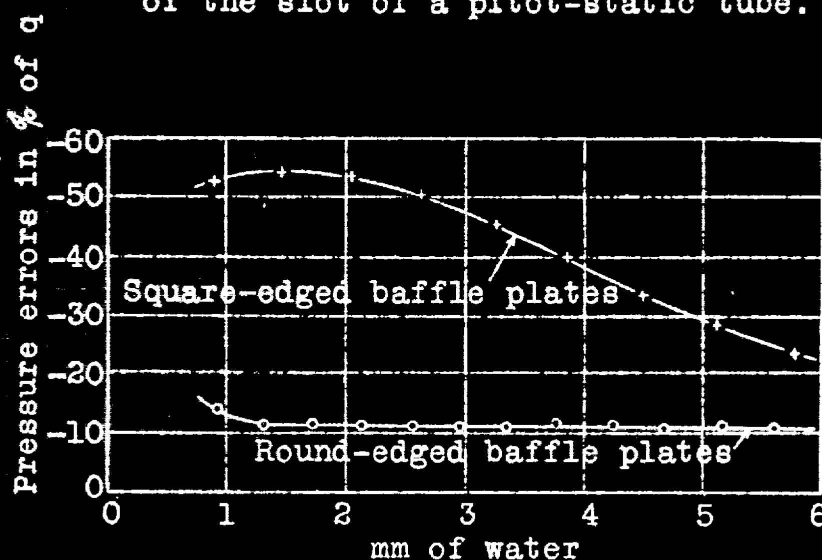

Fig.42 Pressure measurements with transversely placed baffle plates.

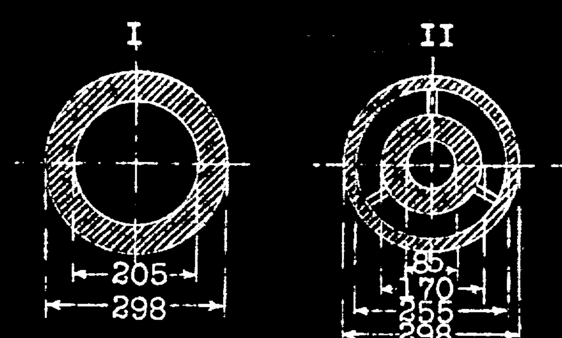

Figs.43 & 44 Turbulence disks.

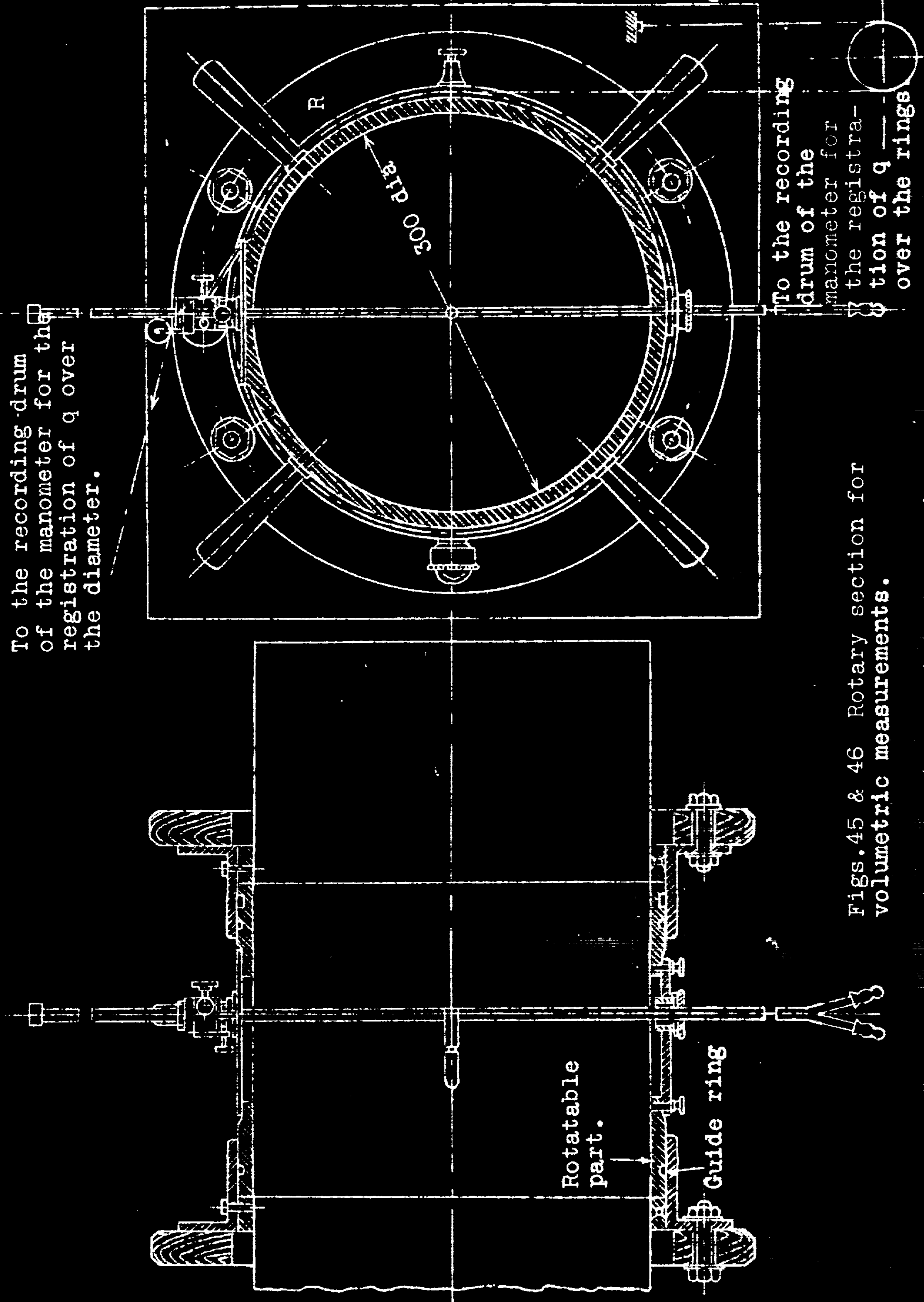

Figs.45 & 46 Rotary section for volumetric measurements.

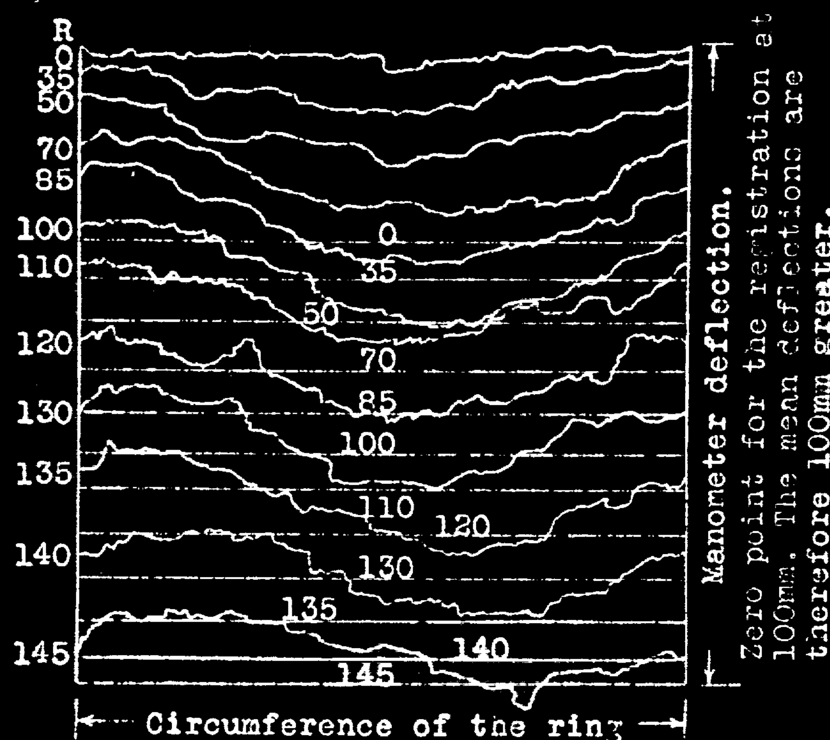

Fig.47 Dynamic pressure curves recorded with the rotary section for Prandtl's pitot-static tube, behind turbulence disk I at medium velocity.

k = Low velocity 0 = Without turbulence disk.
m = Medium velocity 1 = With turbulence disk I
g = High velocity 2 = " " " II

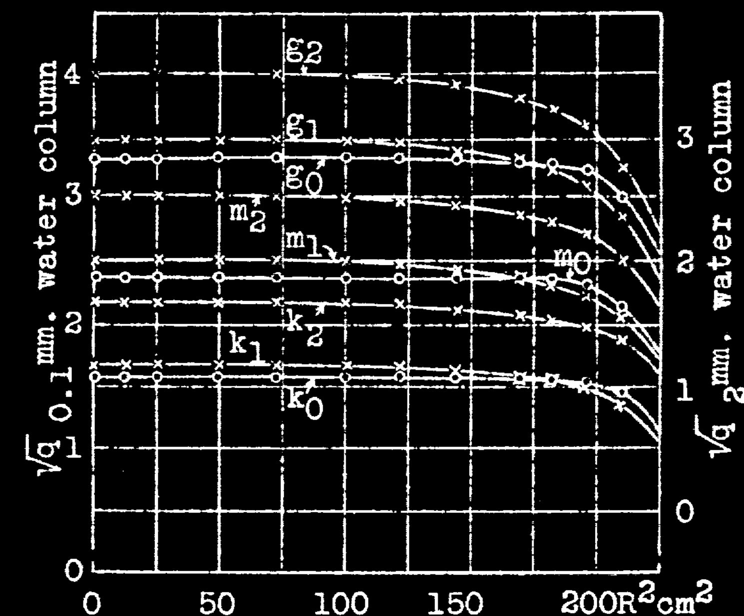

Fig.48 Brabbee's pitot-static tube. Volume measurements with and without turbulence disks.

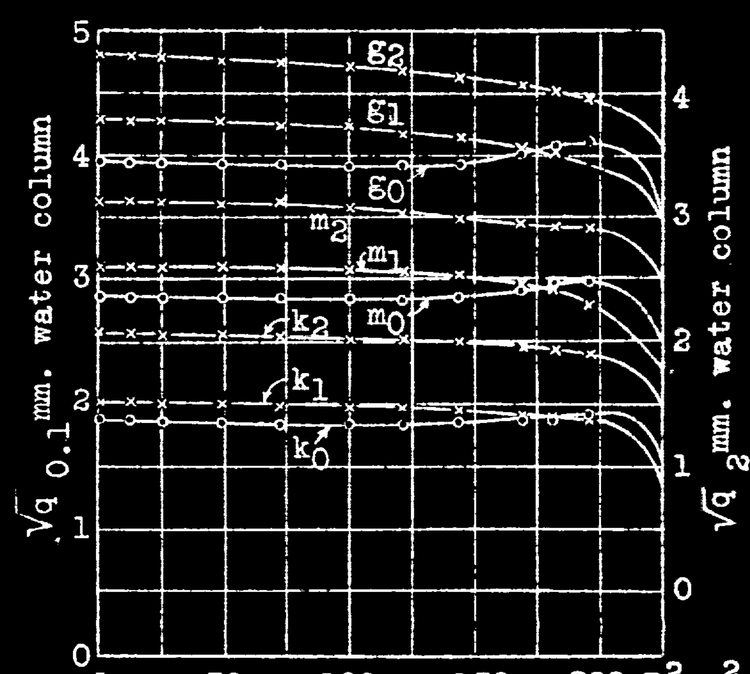

Fig.49 Rounded baffle plates. Volume measurements with and without turbulence disks.

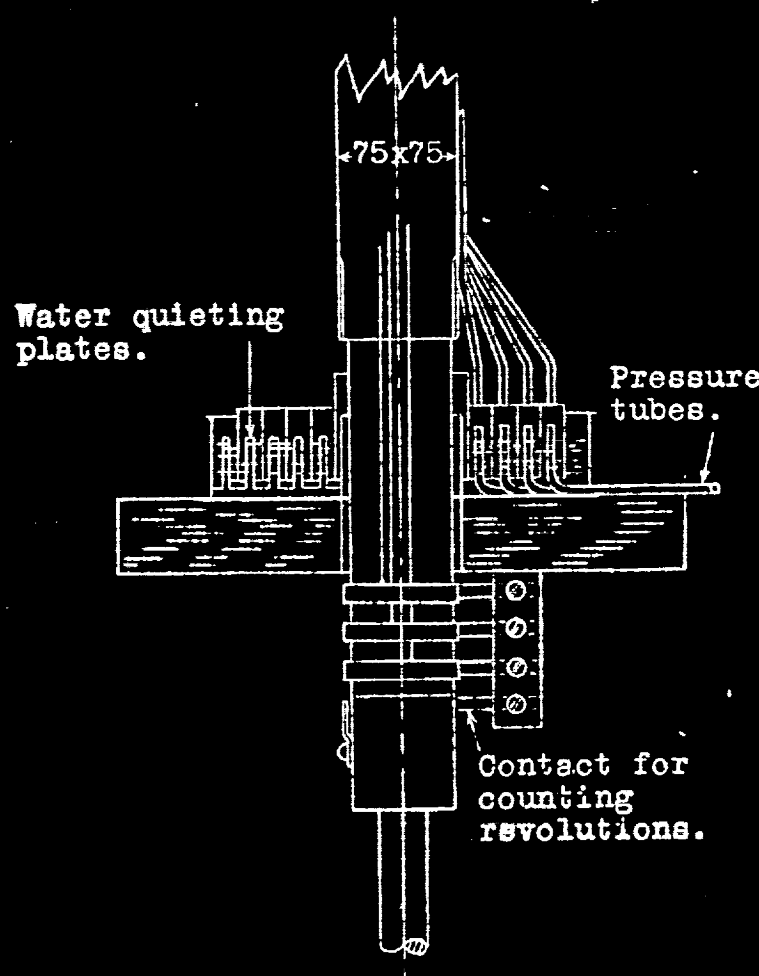

Fig.50 Pressure chamber on whirling arm.